CONTRACT NO. NONR 839(23)
PROJECT NO. NR 064-433

EXPERIMENTAL PRESSURE, TEMPERATURE, AND STRAIN MEASUREMENTS ON ABLATING HEMISPHERICAL NOSE CONES IN HYPERSONIC FLOW TEST SERIES II

by

S. V. Nardo, Burton Erickson and Joseph Kempner

JULY 1961

POLYTECHNIC INSTITUTE OF BROOKLYN

DEPARTMENT
of
AEROSPACE ENGINEERING
and
APPLIED MECHANICS

PIBAL REPORT NO. 574

Contract No. Nonr 839(23)
Project No. NR 064-433

Experimental Pressure, Temperature, and Strain Measurements on Ablating Hemispherical Nose Cones in Hypersonic Flow

Test Series 2

by

S. V. Nardo, Burton Erickson and
Joseph Kempner

Polytechnic Institute of Brooklyn
Department of
Aerospace Engineering and Applied Mechanics

July 1961

PIBAL Report No. 574

TABLE OF CONTENTS

List of Symbols

E	Bridge voltage, m v.
k	Strain gage factor
P	Pressure, psia
P_s	Stagnation pressure, psia
r, φ, θ	Spherical coordinates
s	Circumferential distance, in.
t	Time, secs.
S	Strain gage signal due to stress, m.v.
T	Temperature, ^oF
T_i	Initial temperature, ^oF
T_s	Stagnation temperature, ^oF
T.C., G	Instrument number prefixes, stand for "thermocouple" and "strain gage", respectively
$\Delta R/R$	Unit change of resistance of strain gage
ε	Strain, micro-in./in.

I. Abstract

This report presents the results of pressure, temperature and strain measurements on three hemispherical nose cones tested and ablated in the Polytechnic Institute of Brooklyn hypersonic tunnel. The shrouded model technique, described in Ref. 1, was used in all tests. Wind tunnel stagnation pressure was maintained at a nominal value of 150 psia, and stagnation temperatures varied from 1650 ^{o}R to 1900 ^{o}R. The foregoing test conditions correspond to Mach numbers in the range of 15 to 20, at altitudes of from 60,000 to 70,000 feet.

All three models were fabricated from cast aluminum alloy 356 T-6, and all models had outside diameters of 7-3/4 inches. Two models were 1-inch thick, and the third had a 1/2-inch thickness. Ablation of the surface material was allowed to occur in all tests.

A complete presentation of the data is given in the form of tables, graphs, and photographs.

II. Introduction

In Ref. 2, the data obtained on pressure and temperature measurements of a hemispherical nose cone in the hypersonic tunnel of the Polytechnic Institute of Brooklyn were presented for four different combinations of tunnel stagnation conditions. This nose cone, designated model 1 in the present report, was made of type 304 stainless steel, had a 7-3/4 inch outside diameter, and was one inch thick. The purpose of the tests was to obtain the thermal and aerodynamic loads on the hemispherical configuration with a view to applying this information to analytical studies of transient heat conduction phenomena, and to help formulate techniques for the structural analysis of bodies subject to hypersonic flight environments. The tests on model 1 were the first in a series of tests of an experimental program involving at least a dozen hemispheres with identical external configurations which would be ablated and on which strain measurements would also be undertaken.

The present report gives the results of a second test series involving three hemispherical models. The policy of disseminating the experimental data as they become available, started in Ref. 2, is continued in this presentation. Evaluation of the data in order to obtain heat transfer coefficients and strains, heat conduction studies, together with other topics, will be the subjects of future reports. A two-dimensional transient

heat conduction analysis, based upon the data in Ref. 2, may be found in Ref. 3.

The present report may therefore be considered a continuation of Ref. 2, to which frequent reference will be made. Details of the instrumentation, testing technique, data reduction, and other experimental considerations will be given only when they are different from, or are not undertaken in, the tests on the first model.

The authors gratefully acknowledge the assistance of Messrs. Lawrence D. Brown and Richard F. Parisse for their contribution in the preparation of this report.

III. Models and Instrumentation

Three hemispherical models were tested in the current phase of the experimental program. These models, designated by the numbers 2, 3, and 4, were identical with respect to the material of construction and external configuration. Models 2 and 3 were one-inch thick, but model 4 was 1/2-inch thick. Material of construction, geometry, and type of instrumentation for each model are given in Table 1.

In choosing the material for these models, a simple material which would melt (and ablate) within the stagnation temperature capability of the hypersonic tunnel was desired. Pure aluminum, with a melting range between 1700 to 1830 ^{o}R appeared to be a promising material inasmuch as tunnel stagnation temperatures over 2000 ^{o}R could be realized practically. Because of difficulties in procuring pure aluminum in the required sizes, it was decided to select a cast aluminum alloy. Alcoa alloy 356, heat treated to the T-6 temper, offered a yield stress of approximately 22,000 psi, and hence a reasonable elastic range. Its nominal composition consists of 7% silicon, 0.3% magnesium and approximately 93% aluminum.

Model 2, the first of these cast aluminum alloy hemispheres, was equipped with four pressure taps, nine strain gages, and 29 thermocouples. Pressure taps were included as part of the instrumentation of this model in order to check the aerodynamic loads obtained on the hemispherical stainless steel nose

cone model 1 (Ref. 2). High Temperature Instruments Corporation wire resistance strain gages, designated HT-600, were installed at nine points on the inner (insulated) surface. These strain gages were supplied with individual iron-constantan thermocouples. Twenty additional thermocouples were located at various points throughout the model, bringing the total number of thermocouples to twenty-nine. Fig. 1 shows the location of the various instruments graphically; Table 2 gives the coordinate values, and the orientation of the strain gages.

Details of the method of installing the pressure taps and thermocouples are given in Ref. 2, and will not be repeated here. The only noteworthy difference is the use of aluminum rather than stainless steel for the pressure tubing and the fixtures for the thermocouples. The technique of strain gage installation is outlined below.

The inner surface of the model was prepared in accordance with "Tatnall Measuring Systems Company Bulletin IB-6101". Gages were bonded to the surface at the designated positions with TMS Type H high temperature cement. All gages were cemented and cured to 300°F for four hours before lead extensions were attached. After this preliminary cure, lead extensions of 0.0031 × 1/8 inch glass insulated nichrome ribbon were welded to the strain filament leads in the conventional three wire configuration which provides compensation for lead wire resistance change with temperature variation. Lead extensions were fixed

to the inner surface of the model with TMS type H cement for a length of three inches, and beyond this length they were anchored by 1/2 inch wide strips of No. 27 Scotch electrical tape at two inch intervals.

Thermocouple extensions of 30 gage double glass insulated iron-constantan thermocouple wire were welded to the ends of the thermocouples embedded with the gages and anchored to the inner surface of the specimen in the same manner as the gage extension leads.

All extension leads were brought to the center of the open end of the model where they were collected, together with thermocouples and pressure lines, to form a single cable which was run out from the model mount to recorders.

The fully instrumented model was baked for four additional hours at 300°F to complete the cement cure.

Model 3 instumentation is presented in Fig. 2 and Table 3. Note that this model is identical in geometry with Model 2. There are no pressure taps nor surface thermocouples on Model 3 in order to avoid interference of the instrumentation with the surface ablation of the model during the test run. Another important difference in the instrumentation of this model is the use of HT-1200 strain gages manufactured by the same firm producing the HT-600 gages. Attractive features of the HT-1200 gages, among others, are the linear responses to the temperature variation under stress-free conditions, and the uni-

formity in performance of strain gages from the same lot.

Model 4 is 1/2 inch thick and, as will be noted by referring to Fig. 3 and Table 4, all instruments are located on the insulated surface.

IV. Description of Tests

The hemispherical nose cone models were tested in the shroud rig of the hypersonic tunnel which is described in Ref. 1. A schematic sketch of the model in the shroud tube is shown in Fig. 4.

Minneapolis-Honeywell strip chart recorders were used to record the temperatures, pressures, and strain-gage signals as a function of time. Recorders were also used for the tunnel stagnation pressure and temperature conditions, and to monitor several temperatures at various points in the wind tunnel. The paper speed was 1/3-inch per second for all recorders.

About thirty seconds before the start of the test all recorders were switched on simultaneously and checked to insure that they were running and writing. The pebble bed heater temperature and pressure were adjusted to obtain the desired stagnation pressure and temperature conditions. At the signal to start, the nozzle plug valve was opened. The transient period in which the air flow became steady lasted approximately two to three seconds. The cut-off signal was given when some ablation of the surface had occurred. Simultaneously all recorders were energized to drive the writing pens to one end of the scale in order to assist in establishing the time scale on each chart for data reduction purposes.

V. Reduction of Data

a. Temperatures

All recorders measuring the output of the thermocouples mounted on the models were calibrated to correspond to 1500°F temperature rise for a full scale deflection of 100 divisions. Thus each division corresponded to 15°F temperature rise. The zero setting of the recorders was set at 5 divisions. Inasmuch as the model initial temperatures were within a few degrees of 75°F, zero on the recorder scale was taken as 0°F, and the temperature at any time was obtained by observing the recorder scale reading and multiplying by the calibration constant of 15°F per division. Admittedly, the non-linearity of the thermocouple output would introduce some inaccuracy. Considering the overall accuracy of the recorders (about 1% of full scale) and the immense simplification of data reduction, it was felt that this procedure was justified. An accuracy of the temperatures of $\pm$ 1% of full scale, or $\pm$ 15°F appears conservative in view of the excellent data obtained, but it can be taken as a nominal value.

The time scale was established with little difficulty due to the high conductivity of the aluminum alloy and the apparent uniformity of the nominal speed of all recorders. Time $t = 0$ was easily fixed, even for the buried thermocouple installations, because of the sharp change in slope of the trace at

the time the hypersonic wind tunnel was started. Measurements made of the distance from the point taken as t = 0 to the reference mark made at tunnel cut-off corresponded to periods of time which did not vary by more than one second in the two 83 second test runs, and 1/2 second in the 30 second test run on Model 4. The time scale is thus considered to be within ± 1/2 second of the values given in the tables and graphs.

b. Pressures

Only one of the three models tested was equipped with pressure taps. The pressure tap tubing was connected to Statham pressure transducers, and then the transducer output was impressed on the input terminals of a recorder. There was no difficulty in establishing the time scale for the pressure records. Accuracy of the data is estimated at ± 1% of full scale.

c. Strain Gage Data

The strain gages responded almost instantaneously to the aerodynamic loading, thus time t = 0 was easily established. From the temperature-time records of the thermocouples, either embedded with the gages or from thermocouples on the insulated surface at the same latitude, the strain gage output in millivolts could be obtained as a function of the temperature. Laboratory calibration tests on both types of strain gages yielded the unit change of resistance vs. temperature for stress-free conditions. In principle, therefore, the strain gage response to

stress could be obtained by subtracting the stress-free calibration response from the response during the test run, at the same temperature. Finally, the response due to stress could be converted to strain from a knowledge of the strain gage factor at various temperatures.

The stress-free response of the gages was obtained by a special laboratory testing technique. Strain gages were affixed to samples of 356 T-6 aluminum alloy in precisely the same manner as they were subsequently affixed to the models. The samples were placed into an oven, and simultaneous readings were taken of the strain gage output and temperature. Typical results are shown in Figs. 5 and 6a. Heating rates varied from 0.2 to 0.3 ^{o}F/sec. Inasmuch as no constraints were placed on the samples, the strain gage output corresponded to the stress-free response of the assembly as a function of temperature. It was assumed that this response was independent of the heating rate.

Reduction of the strain gage data is outlined in the following steps.

(1) From the wind-tunnel test, strain gage output is obtained as a function of time.

(2) From thermocouples embedded in the strain gages (or installed near the gage) a temperature-time history at the gage location is obtained.

(3) Combining (1) and (2), the strain-gage output is

obtained as a function of temperature.

(4) Subtracting the stress-free strain gage output from the output (3) at the same temperature yields the strain gage output due to stresses.

(5) From data on the gage factor as a function of temperature, the strain can be obtained. The strain as a function of time can of course be prepared from the original temperature-time history at the gage location.

It should be noted that the strain data presented is due to the combination of the external surface loads, and to thermal stresses arising from temperature variations in the body and edge constraints.

One final note in connection with the reduction of strain gage data should be made for the HT-1200 strain gages. Under conventional conditions of use, the stress-free response of these gages over large ranges of temperature change is both linear and large (Fig. 6a). A circuit was designed to reduce this output to the same magnitude as that of the embedded I.C. thermocouple associated with the gage. Since both of these responses to temperature change are substantially linear and can be equally matched by trial, the output of the thermocouple can be used to balance the simple temperature component of the strain gage response, resulting in almost zero sensitivity of the gage

to temperature change. Laboratory stress-free calibration tests on the HT-1200 strain gages, using the attenuating circuit described, are presented in Fig. 6b.

VI. Presentation of Data

In this section, the data obtained on pressure, temperature, strain and ablation is presented in tabular and graphical form. The model geometry, identification numbers, and instrumentation for the three aluminum alloy hemispherical nose cone configurations are shown in Table 1. In Table 5 are noted the tunnel stagnation temperature and pressure conditions, duration of test, and remarks on the degree of ablation. It is emphasized that tunnel stagnation conditions quoted in the table are nominal values; variation in these conditions with time are presented in the tabular and graphical data presented for each model. The instruments on each model are identified by number and letter symbols. Instrument location is shown graphically in Figs. 1, 2 and 3, and in tabular form, Tables 2, 3, and 4. These latter tables also present information on the instruments which were connected to recorders, those which failed prior or during the test, and other pertinent remarks. Model 2, for example, had more instruments than available recorders, and hence a number of thermocouples could not be utilized during the test run.

Data are presented in this section in such a manner that the same physical quantity is shown in a group for all three models.

a. Tunnel Stagnation Conditions

Stagnation pressure and temperature conditions for

each of the three tests are presented in Fig. 7 as a function of time. These data are obtained from a rake mounted ahead of the test section which contains two temperature and two pressure probes (Fig. 4). Two probes of each type are installed on the rake in case one of the instruments should fail. Unfortunately, both temperature probes were damaged prior to the test on Model 3, and no stagnation temperature is available for this test run. The initial heater pressure and temperature for the test run on Model 4 approximated those for the test run on Model 3, and an approximation for Model 3 stagnation temperature may be taken from the data for Model 4.

b. Pressures

As was mentioned previously, only Model 2 was equipped with pressure taps. The pressure distribution or aerodynamic loading had been established on Model 1 and reported in Ref. 2. It was considered desirable, however, to install a few pressure taps to double check the previous data. Table 6 gives the pressure data as a function of time. These data are plotted in Fig. 8 as a ratio of the stagnation pressure versus latitude. At any particular latitude, the plotted pressure ratio is an average value taken at various times over the entire test run. Maximum deviation from this average value was about 12 percent for pressure tap 4, which was recording the lowest pressures. For the other pressure taps the corresponding value was 4 percent. Also shown in Fig. 8 is a curve corresponding to the

Newtonian approximation for the hemisphere in the shroud. Additional pressure data appears in Fig. 22 of Ref. 2. In subsequent theoretical work, the pressure distribution can be obtained graphically by fairing a curve through the experimental points, or by fitting an appropriate function to the test data by the method of least squares.

c. Temperatures

Temperature data as a function of time is presented in Tables 7, 8 and 9 for Models 2, 3 and 4, respectively. The tabulated data gives the time (t) in seconds and the corresponding temperatures (T) in degrees Fahrenheit for all thermocouples, including the stagnation temperature. For convenience, the temperature is also given in the non-dimensional form $(T_s - T)/(T_s - T_i)$, where the subscripts s and i stand for stagnation and initial temperatures, respectively. Also indicated in these tables is the full scale deflection setting, or sensitivity of the recorders, in degrees Fahrenheit.

In Figs. 9 to 13 the thermocouple data have been plotted for selected points on the various models tested. Figs. 9 and 10 give temperature-time histories through the thickness and at a fixed radial position at various points along a meridian for Model 2. Plots of temperature versus meridional distance for various fixed times are shown for all models in Figs. 11, 12 and 13.

d. Strain Gage Data

Model 2 was equipped with nine HT-600 high temperature strain gages in the manner already described. Just prior to the test run a leak occurred in the high pressure water line which cools the walls of the shroud tube. Although only a small amount of water collected at the bottom of the tunnel wall, the combination of high humidity and the hygroscopic nature of the strain gage cement shorted all the gages to ground. The excess water was drained off and the model was warmed up to about 250°F several times in an attempt to dry out the cement. This technique appeared to restore four strain gages to working order. An examination of the records after the test run, however, showed such erratic behavior that no data are available for these gages.

A measure of success was achieved in Models 3 and 4 which were equipped with HT-1200 strain gages. The data from Model 3 were erratic and are not presented. The stress-free unbiased calibration curves are shown in Fig. 6a. The response is essentially linear, with an average slope of $122 \times 10^{-6}/^{\circ}F$. The output of the sensing circuits of the HT-1200 were biased by means of the signal from the embedded thermocouples. The net effect was to reduce the stress-free response of the gages to that of Fig. 6b. Using the procedure outlined in Section V, the strain as a function of time was obtained. These results are plotted in

Fig. 14. Intermediate steps are not shown. At a given temperature, the strain gage signal S due to stress was converted to strain through the use of the expression

$$\varepsilon = 4S/Ek$$

where

ε = strain

E = bridge voltage, m.v.

k = gage factor

S = signal due to stress, m.v.

In reducing the data to strain, a constant strain gage factor of 3.2 was used. This gage factor was the average value obtained in tests at various temperatures conducted at the National Bureau of Standards (NBS Report 6900, Table 2).

It is emphasized that the results discussed above are tentative; they represent the best response obtained after successively better trials.

e. Ablation

A photograph of Model 2 prior to testing is shown in Fig. 15. Since all three models were designed to the same external configuration and constructed of the same material, pretest photographs of Models 3 and 4 would have been identical.

Model 2, the first hemisphere tested, was only mildly ablated. Photographic views of Model 2 after testing are shown in Fig. 16. The test was conducted at a stagnation pressure of

approximately 155 psia and a stagnation temperature of about 1150°F; the test duration was 83 seconds. The aluminum alloy melted near the stagnation point and resolidified as it was carried along the model meridians. Along the meridian that contained the pressure taps, the depth of the ablation was more pronounced, and a greater amount of resolidified material was in evidence. It was also noted that at time t = 55 seconds, pressure tap number 3, at an angle $\theta = 50^{\circ}$ from the stagnation point, behaved peculiarly, indicating that molten aluminum had wholly or partially obstructed the opening. Examination of Model 2, after the test, showed that resolidified material had indeed been deposited on the static tap opening.

Photographic views of Models 3 and 4 are presented in Figs. 17 and 18, respectively. The extent of ablation of Model 3 is much more pronounced than on Model 2. On Model 4 the combination of air loads, high temperature, and ablation resulted in the formation of a hole which penetrated the entire thickness at the hemisphere.

VII. Concluding Remarks

Subsequent models in this test series will have the instrumentation only on the inner surfaces, to avoid interference with the ablation on the heated surface. It is therefore essential that the temperatures throughout the model be known as a function of time. From the data obtained on Models 1 and 2, and from theoretical and empirical data available on the subject, heat transfer coefficients can be established for any combination of wind tunnel stagnation conditions. Various heat conduction analyses will then be applied and the resulting temperature distributions compared with the temperature data obtained on Models 1 and 2. If satisfactory agreement is obtained, the temperature distributions on all hemispherical nose cone configurations can be predicted. The data presented in Ref. 2 and in this report are currently being evaluated to achieve this objective.

By far the most difficult of the measurements will be associated with the transient strains. The HT-600 gages installed on Model 2 do not appear promising. Although no sensible data were obtained from these gages during the test run on Model 2, this conclusion is based upon the erratic behavior of the stress-free laboratory tests conducted on these gages (Fig. 5). The performance of the HT-1200 gages, however, is considerably better. Various techniques of moisture-proofing the gage instal-

lations are being evaluated to avoid the difficulties experienced in this series of tests. A separate report covering the evaluation, installation, performance, and data reduction of the high temperature strain gages used in this project will be published in the future.

Measurements of the degree of ablation on the surfaces have been made; the models have also been sectioned and prepared for metallurgical examination. This information will be included in future PIBAL reports.

References

1. Ferri, Antonio and Libby, Paul A.: The Hypersonic Facility of the Polytechnic Institute of Brooklyn and its Application to Problems of Hypersonic Flight, WADC TR 57-369, ASTIA Document No. AD 130 809, August 1957.

2. Nardo, S. V., Boccio, John L., Erickson, Burton, and Kempner, Joseph: Experimental Temperature Distribution in a Hemispherical Nose Cone in Hypersonic Flow, PIBAL Report No. 494, June 1959.

3. Pohle, Frederick V. and Boccio, John L.: Transient Temperature Distributions in a Sphere due to Aerodynamic Heating, PIBAL Report No. 553, September 1959.

TABLE 1

Model Geometry and Instrumentation

Model No.	Material	External Diameter, In.	Wall Thickness, In.	Pressure Taps	Thermo-Couples[a]	Strain Gages
2	Cast Aluminum Alloy 356 T-6	7-3/4	1	4	29	9 (HT-600)
3		7-3/4	1	0	24	9 (HT-1200)
4		7-3/4	1/2	0	23	11 (HT-1200)

(a) Includes thermocouples built into the high temperature strain gages.

TABLE 2

LOCATION OF INSTRUMENTS

MODEL 2

Instrument Number	Instrument	θ Degrees	φ Degrees	R Inches	Remarks
P-1	Pressure Tap	15	225	3.875	
P-2	↓	30	↓	↓	
P-3	↓	50	↓	↓	Blocked by Ablating Material After 55 Sec.
P-4	↓	70	↓	↓	
P-S	↓	Upstream from Model			
1(H)	Thermocouple	15	0	3.875	
2(H)	↓	30	↓	↓	
3(H)	↓	45	↓	↓	
4(H)	↓	60	↓	↓	
5(H)	↓	75	↓	↓	Unsatisfactory Junction
6(B)	↓	15	30	3.625	
7(B)	↓	30	60	↓	
8(B)	↓	45	30	↓	
9(B)	↓	60	30	↓	
10(B)	↓	75	30	↓	
11(B)	↓	15	60	3.375	
12(B)	↓	30	75	↓	
13(B)	↓	45	60	↓	
14(B)	↓	60	60	↓	*
15(B)	↓	75	60	↓	

TABLE 2 (Concluded)

LOCATION OF INSTRUMENTS

MODEL 2

Instrument Number	Instrument	ϑ Degrees	φ Degrees	R Inches	Remarks
16(I)	Thermocouple	15	90	2.875	*
17(I)		30			*
18(I)		45			*
19(I)		60			*
20(I)		75			
T1(I)		0	0		
T2(I)		15	135		Recorder not Operating After 22 Seconds
T3(I)		15			*
T4(I)		35			
T5(I)		35			*
T6(I)		55			
T7(I)					*
T8(I)			315		*
T9(I)			315		*
G1	Strain Gage	0	0		(b)
G2		15	135		ϑ direction (a)
G3		15			φ " (b)
G4		35			ϑ " (a)
G5		35			φ " (b)
G6		55			ϑ " (a)
G7					φ " (a)
G8			315		ϑ " (a)
G9			315		φ " (a)

(H) Heated Surface
(B) Buried Surface
(I) Insulated Surface

* Not in use = Insufficient number of recorders
(a) Gage shorted to ground - humidity
(b) Data unsatisfactory

TABLE 3

LOCATION OF INSTRUMENTS

MODEL 3

Instrument Number	Instrument	ϑ Degrees	φ Degrees	R Inches	Remarks
1(I)	Strain Gage Thermocouple	0	135	2.875	
2	↓	15	↓	↓	(a)
3	↓	15	↓	↓	↓
4	↓	35	↓	↓	↓
5	↓	35	↓	↓	↓
6	↓	55	↓	↓	↓
7	↓	55	135	↓	↓
8	↓	55	315	↓	↓
9(I)	↓	55	315	2.875	(a)
10(B)	Thermocouple	15	30	3.625	
11	↓	30	↓	↓	Erratic
12	↓	45	↓	↓	↓
13	↓	60	↓	↓	↓
14	↓	75	30	3.625	↓
15	↓	15	60	3.375	↓
16	↓	30	↓	↓	↓
17	↓	45	↓	↓	↓
18	↓	60	↓	↓	↓
19(B)	↓	75	60	3.375	↓
20(I)	↓	15	90	2.875	↓
21	↓	30	↓	↓	↓
22	↓	45	↓	↓	↓
23	↓	60	↓	↓	↓
24(I)	↓	75	90	2.875	↓

TABLE 3 (Concluded)

LOCATION OF INSTRUMENTS

MODEL 3

Instrument Number	Instrument	ϑ Degrees	φ Degrees	R Inches	Remarks
G1	Strain Gage	0	135	2.875	
G2	"	15	"	"	φ Direction
G3	"	15	"	"	ϑ "
G4	"	35	"	"	φ "
G5	"	35	"	"	ϑ "
G6	"	55	"	"	φ "
G7	"	55	135	"	ϑ "
G8	"	55	315	"	φ " (b)
G9	"	55	315	"	ϑ " (b)

(H) Heated Surface
(B) Buried Surface
(I) Insulated Surface
(a) Used to bias output of respective strain gage
(b) Shorted to ground-humidity

TABLE 4

LOCATION OF INSTRUMENTS

MODEL 4

Instrument Number	Instrument	ϑ Degrees	φ Degrees	Remarks
1	Strain Gage Thermocouple	0	0	(a)
2	″	15	″	″
3	″	15	″	″
4	″	30	″	″
5	″	30	″	″
6	″	45	″	″
7	″	45	″	″
8	″	55	″	″
9	″	55	0	″
10	″	45	180	″
11	″	45	180	(a)
12	Thermocouple	0	270	
13	″	0	90	
14	″	15	270	
15	″	15	90	
16	″	30	270	
17	″	30	90	
18	″	45	270	
19	″	45	90	
20	″	55	270	
21	″	55	90	
22	″	30	180	
23	″	55	180	No Record

TABLE 4 (Concluded

LOCATION OF INSTRUMENTS

MODEL 4

Instrument Number	Instrument	ϑ Degrees	φ Degrees	Remarks
G1	Strain Gage	0	0	
G2		15		φ Direction
G3		15		ϑ "
G4		30		φ "
G5		30		ϑ "
G6		45		φ "
G7		45		ϑ "
G8		55	↓	φ "
G9		55	0	ϑ "
G10		45	180	φ "
G11	↓	45	180	ϑ "

All instrumentation on insulated surface, R = 3.375 in.
(a) Used to bias output of respective strain gage.

TABLE 5

SUMMARY OF TUNNEL STAGNATION CONDITIONS, TEST DURATION AND DEGREE OF ABLATION

Model	Stagnation Pressure, psia*	Stagnation Temperature °F*	Duration of Test Seconds	Degree of Ablation
2	155	1150	84	mild
3	155	--	80	severe
4	150	1450	30	very severe

*Listed values of stagnation pressure and stagnation temperature are nominal values.

TABLE 6

PRESSURE-TIME HISTORIES

Model 2 — Pressure in psia

Time Seconds	Stagnation Pressure P_s	P_1	P_1/P_s	P_2	P_2/P_s	P_3	P_3/P_s	P_4	P_4/P_s
6	144	138	0.958	122	0.847	72.6	0.505	16.5	0.115
12	146	140	0.960	124	0.850	74	0.506	16.3	0.112
18	148	142	0.958	125	0.843	75	0.506	16.1	0.109
24	150	144	0.958	126	0.838	76	0.506	15.9	0.106
30	152	145.5	0.956	127.5	0.839	76.8	0.506		0.105
36	154	147	0.954	129	0.836	77.6	0.504		0.104
42	156	149.5	0.958	131	0.839	79	0.506		0.102
48	157	(a)	-	132	0.839	80	0.509		0.101
54	158		-	133	0.840	80.5	0.509		0.101
60	159		-	134	0.841	(b)	-		0.100
66	160		-	134	0.837		-		0.0994
72	160.5		-	133	0.827		-		0.0990
78	161		-	130	0.806		-		0.0986
83	165	↓	-	135	0.817	↓	-	↓	0.0962
Average P/P_s:			0.957		0.836		0.506		0.103

(a) Off scale.

(b) Pressure tap clogged at t = 55 seconds.

TABLE 7

TEMPERATURE-TIME HISTORIES

MODEL NO. 2

Time	Thermocouple Number								
	T_s	1		2		3		4	
Seconds	°F	T(°F)	$\frac{T_s-T}{T_s-T_i}$	T(°F)	$\frac{T_s-T}{T_s-T_i}$	T(°F)	$\frac{T_s-T}{T_s-T_i}$	T(°F)	$\frac{T_s-T}{T_s-T_i}$
0	75	75	1.000	75	1.000	75	1.000	75	1.000
1.5	543	153	0.833	167	0.803	152	0.835	133	0.876
3	811	214	0.811	240	0.776	225	0.796	180	0.857
5	911	280	0.755	305	0.725	315	0.713	233	0.811
10	991	416	0.628	449	0.580	438	0.604	326	0.726
15	1010	530	0.513	545	0.487	525	0.523	433	0.642
20	1056	620	0.444	634	0.430	610	0.455	486	0.581
30	1100	770	0.322	760	0.332	732	0.359	608	0.480
40	1143	880	0.246	860	0.265	828	0.295	706	0.409
50	1175	963	0.193	948	0.206	902	0.243	798	0.343
60	1197	1028	0.151	1000	0.176	968	0.204	870	0.291
70	1215	1080	0.118	1042	0.152	1013	0.177	922	0.257
84	1225	1090	0.117	1080	0.126	1045	0.156	974	0.218
Full Scale	1815	1500		1500		1500		1500	

T_i = Initial Temperature, 75°F

T_s = Stagnation Temperature, °F

TABLE 7 (Continued)

TEMPERATURE-TIME HISTORIES

MODEL No. 2

Time	Thermocouple Number							
	6		7		8		9	
Seconds	T(°F)	$\frac{T_s-T}{T_s-T_i}$	T(°F)	$\frac{T_s-T}{T_s-T_i}$	T(°F)	$\frac{T_s-T}{T_s-T_i}$	T(°F)	$\frac{T_s-T}{T_s-T_i}$
0	75	1.000	75	1.000	75	1.000	75	1.000
1.5	120	0.904	127	0.889	136	0.870	118	0.908
3	174	0.865	180	0.857	191	0.842	150	0.898
5	229	0.814	232	0.791	241	0.803	198	0.852
10	365	0.683	390	0.656	361	0.689	298	0.756
15	483	0.562	499	0.548	473	0.575	385	0.668
20	583	0.472	584	0.479	561	0.506	464	0.604
30	743	0.347	723	0.368	695	0.396	588	0.498
40	846	0.278	826	0.295	796	0.326	692	0.422
50	926	0.225	908	0.242	872	0.275	783	0.355
60	992	0.184	979	0.195	932	0.237	857	0.305
70	1042	0.152	1025	0.166	981	0.206	910	0.268
84	1079	0.128	1057	0.147	1032	0.168	960	0.230
Full Scale	1500		1500		1500		1500	

TABLE 7 (Continued)

TEMPERATURE-TIME HISTORIES

MODEL NO. 2

Time	Thermocouple Number							
	10		11		12		13	
Seconds	T(°F)	$\frac{T_s-T}{T_s-T_i}$	T(°F)	$\frac{T_s-T}{T_s-T_i}$	T(°F)	$\frac{T_s-T}{T_s-T_i}$	T(°F)	$\frac{T_s-T}{T_s-T_i}$
0	75	1.000	75	1.000	75	1.000	75	1.000
1.5	89	0.970	110	0.925	111	0.923	110	0.925
3	104	0.961	147	0.902	153	0.894	151	0.897
5	127	0.938	206	0.842	221	0.826	212	0.834
10	199	0.864	344	0.707	369	0.679	346	0.703
15	273	0.788	459	0.588	478	0.567	447	0.596
20	343	0.727	557	0.509	570	0.496	528	0.529
30	472	0.613	715	0.376	716	0.375	666	0.416
40	584	0.522	834	0.290	826	0.297	773	0.346
50	683	0.447	916	0.235	908	0.243	857	0.289
60	767	0.391	977	0.197	972	0.200	922	0.247
70	829	0.338	1031	0.162	1026	0.165	977	0.213
84	888	0.293	1072	0.133	1063	0.141	1030	0.171
Full Scale	1500		1500		1500		1500	

TABLE 7 (Continued)

TEMPERATURE-TIME HISTORIES

MODEL NO. 2

Time	Thermocouple Number							
	15		20		T1		T2	
Seconds	T(°F)	$\frac{T_s-T}{T_s-T_i}$	T(°F)	$\frac{T_s-T}{T_s-T_i}$	T(°F)	$\frac{T_s-T}{T_s-T_i}$	T(°F)	$\frac{T_s-T}{T_s-T_i}$
0	75	1.000	75	1.000	75	1.000	75	1.000
1.5	83	0.983	73	0.994	169	0.799	90	0.968
3	98	0.969	89	0.981	234	0.784	115	0.946
5	120	0.946	111	0.956	292	0.739	171	0.885
10	189	0.874	187	0.880	413	0.631	314	0.739
15	261	0.801	260	0.802	520	0.523	433	0.617
20	330	0.740	331	0.740	609	0.456	527	0.539
30	453	0.631	456	0.628	758	0.335		
40	563	0.543	565	0.542	878	0.248		
50	659	0.470	662	0.466	973	0.184		
60	740	0.407	748	0.400	1033	0.146		
70	806	0.359	812	0.354	1060	0.136		
84	873	0.306	880	0.300	1081	0.126		
Full Scale	1500		1500		1500		1500	

TABLE 7 (Concluded)

TEMPERATURE-TIME HISTORIES

MODEL NO. 2

Time	Thermocouple Number			
	T_4		T_6	
Seconds	$T(^{\circ}F)$	$\frac{T_s-T}{T_s-T_i}$	$T(^{\circ}F)$	$\frac{T_s-T}{T_s-T_i}$
0	75	1.000	75	1.000
1.5	100	0.947	93	0.962
3	140	0.912	122	0.936
5	199	0.853	165	0.895
10	328	0.726	275	0.783
15	423	0.629	362	0.693
20	511	0.556	442	0.626
30	643	0.447	578	0.509
40	758	0.361	694	0.420
50	853	0.293	783	0.356
60	923	0.245	855	0.306
70	978	0.209	908	0.270
84	1016	0.186	969	0.222
Full Scale	1500		1500	

TABLE 8

TEMPERATURE-TIME HISTORIES

MODEL 3

Time	Thermocouple Number					
	10	11	12	13	14	15
Seconds	T(°F)	T(°F)	T(°F)	T(°F)	T(°F)	T(°F)
0	75	75	75	75	75	75
1.5	149	154	165	120	85.5	105
3.0	213	231	225	171	105	158
4.5	278	300	290	212	131	220
6.0	339	360	345	255	158	285
7.5	394	418	390	292	180	345
9.0	444	465	434	326	210	398
12.0	530	545	504	390	262	495
15.0	607	615	564	444	315	578
18.0	675	675	615	495	368	651
21.0	730	725	668	540	413	710
24.0	780	765	713	585	456	758
30.0	855	835	784	656	533	840
36.0	915	894	846	720	605	900
42.0	961	944	893	780	667	952
48.0	1005	(a)	940	830	724	995
54.0	1040		983	870	776	1035
60.0	1060		1020	908	818	1060
66.0	1062		1050	970	864	1065
72.0	1065		1065	1010	915	1070
78.0	1065	↓	1070	1035	970	1070
80.0	1065	1070	1070	1040	970	1070
Full Scale	1500	1500	1500	1500	1500	1500

TABLE B (Cont'd)

TEMPERATURE-TIME HISTORIES

MODEL 3

Time	Thermocouple Number						
	16	17	18	19	20	21	22
Seconds	T(°F)	T(°F)	T(°F)	T(°F)	T(°F)	T(°F)	T(°F)
0	75	75	75	75	75	75	75
1.5	119	116	111	84	120	115	115
3.0	186	175	153	100	183	180	168
4.5	255	240	185	118	246	247	225
6.0	319	300	240	143	303	315	284
7.5	371	353	278	176	363	366	332
9.0	424	400	316	204	414	419	377
12.0	507	480	384	253	502	505	470
15.0	580	547	441	306	579	577	525
18.0	645	607	489	357	649	640	583
21.0	698	675	536	405	709	697	634
24.0	750	730	579	452	760	745	678
30.0	820	770	660	530	835	816	757
36.0	880	834	724	603	894	879	817
42.0	932	884	780	666	945	930	870
48.0	975	935	832	721	990	975	915
54.0	1015	968	876	772	1025	1010	959
60.0	1050	1000	908	814	1050	1050	1000
66.0	1060	1030	960	854	1060	1060	1025
72.0	1065	1050	1005	904	1065	1065	1050
78.0	1070	1055	1030	950	1065	1070	1065
80.0	1072	1060	1030	954	1065	1070	1066
Full Scale	1500	1500	1500	1500	1500	1500	1500

TABLE 8 (Concluded)

TEMPERATURE-TIME HISTORIES

MODEL 3

Time	Thermocouple Number			
	23	24	8	9
Seconds	T(°F)	T(°F)	T(°F)	T(°F)
0	75	75	75	75
1.5	85.5	90	112	99.4
3.0	115	112	158	130
4.5	172	138	204	173
6.0	218	165	248	210
7.5	252	193	291	249
9.0	285	222	325	285
12.0	360	273	396	348
15.0	420	324	456	405
18.0	483	375	504	457
21.0	520	420	550	503
24.0	562	460	595	547
30.0	642	536	668	626
36.0	717	607	735	694
42.2	770	670	790	750
48.0	817	724	835	802
54.0	866	768	877	844
60.0	900	814	915	880
66.0	950	844	955	925
72.0	997	888	1000	980
78.0	1026	930	1040	1020
80.0	1030	940	1040	1020
Full Scale	1500	1500	1500	1500

Note: Stagnation temperature data was not obtained due to break in thermocouple wires.

(a) Erratic in this time interval.

TABLE 9

TEMPERATURE-TIME HISTORIES

MODEL 4

Time	Thermocouple Number															
	T_s	12		13		14		15		16		17		18	
Seconds	(^oF)	T(^oF)	$\frac{T_s-T}{T_s-T_i}$	T(^oF)	$\frac{T_s-T}{T_s-T_i}$	T(^oF)	$\frac{T_s-T}{T_s-T_i}$	T(^oF)	$\frac{T_s-T}{T_s-T_i}$	T(^oF)	$\frac{T_s-T}{T_s-T_i}$	T(^oF)	$\frac{T_s-T}{T_s-T_i}$	T(^oF)	$\frac{T_s-T}{T_s-T_i}$
0	90	90	1.000	90	1.000	85	1.000	90	1.000	90	1.000	90	1.000	90	1.000
1.5	1045	165	0.922	168	0.918	179	0.907	188	0.897	218	0.866	218	0.866	204	0.881
3	1285	263	0.855	255	0.862	284	0.838	292	0.831	345	0.787	336	0.794	322	0.806
4.5	1375	353	0.795	354	0.795	382	0.773	382	0.773	450	0.720	443	0.725	428	0.737
6	1410	442	0.733	449	0.728	472	0.711	473	0.710	541	0.658	535	0.663	510	0.682
9	1421	586	0.627	585	0.627	622	0.600	615	0.606	682	0.555	678	0.558	653	0.577
12	1445	720	0.535	720	0.535	742	0.519	742	0.519	795	0.480	795	0.480	750	0.513
15	1460	825	0.464	820	0.467	840	0.453	840	0.453	884	0.420	878	0.425	834	0.457
18	1480	908	0.412	900	0.417	920	0.403	915	0.406	946	0.384	945	0.385	895	0.421
21	1500	971	0.375	975	0.372	984	0.366	983	0.366	1005	0.351	1000	0.355	945	0.394
24	1525	1035	0.342	1030	0.345	1030	0.345	1035	0.342	1045	0.334	1040	0.337	995	0.369
27	1520	1051	0.328	1050	0.329	1050	0.329	1055	0.325	1060	0.308	1050	0.329	1035	0.339
30	1480	1065	0.299	1055	0.306	1052	0.308	1060	0.302	1065	0.299	1058	0.304	1055	0.306
Full Scale	1625	1500		1500		1500		1500		1500		1500		1500	

TABLE 9 (Concluded)

TEMPERATURE-TIME HISTORIES

MODEL 4

Time Seconds	Thermocouple Number 19		20		21		22	
	$T(^{o}F)$	$\frac{T_s-T}{T_s-T_i}$	$T(^{o}F)$	$\frac{T_s-T}{T_s-T_i}$	$T(^{o}F)$	$\frac{T_s-T}{T_s-T_i}$	$T(^{o}F)$	$\frac{T_s-T}{T_s-T_i}$
0	90	1.000	90	1.000	90	1.000	90	1.000
1.5	213	0.871	168	0.918	195	0.890	218	0.866
3	333	0.797	261	0.857	290	0.833	339	0.792
4.5	441	0.727	345	0.802	368	0.784	453	0.718
6	525	0.670	414	0.755	443	0.733	545	0.655
9	659	0.573	533	0.667	560	0.647	690	0.549
12	765	0.502	623	0.607	645	0.590	803	0.474
15	845	0.449	705	0.551	721	0.539	885	0.420
18	904	0.420	769	0.512	787	0.499	955	0.378
21	958	0.384	825	0.479	845	0.465	1010	0.348
24	1000	0.366	875	0.453	890	0.443	1050	0.331
27	1035	0.339	923	0.417	934	0.410	1058	0.323
30	1052	0.308	995	0.349	1000	0.345	1065	0.299
Full Scale	1500		1500		1500		1500	

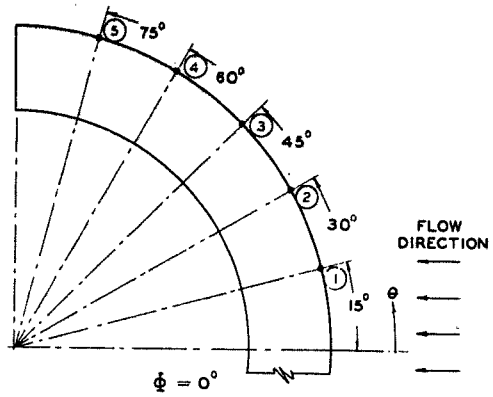

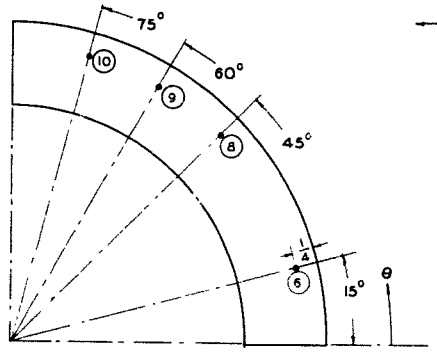

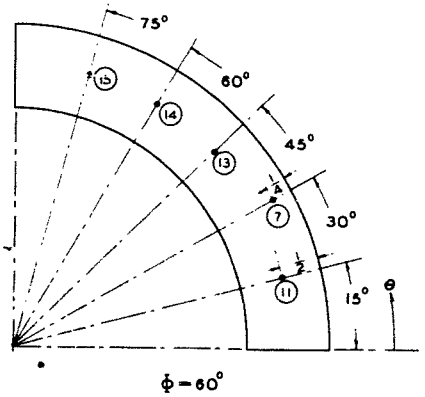

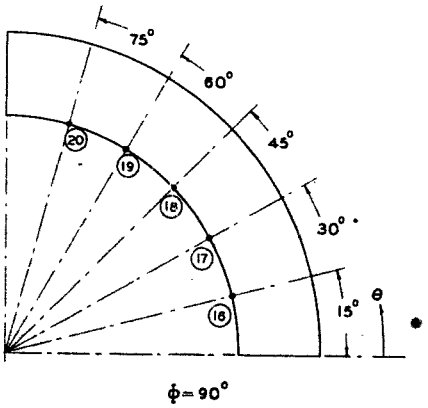

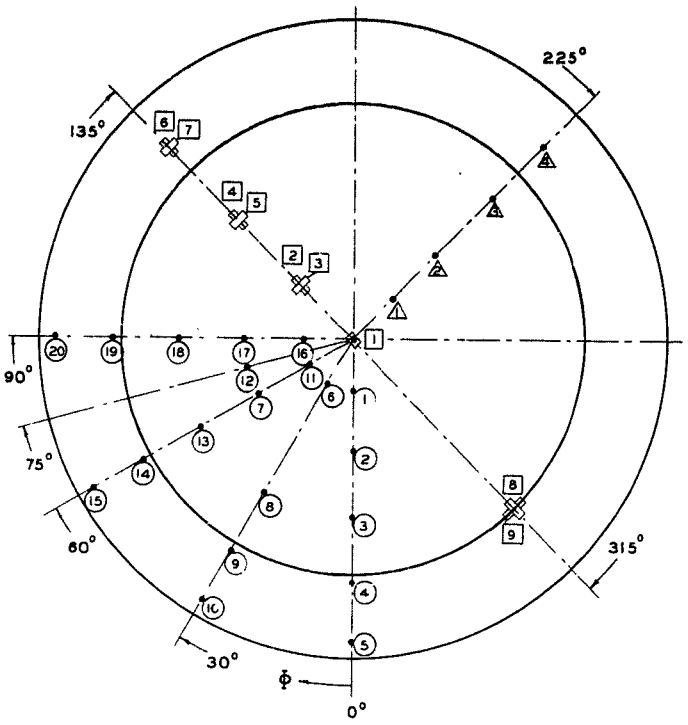

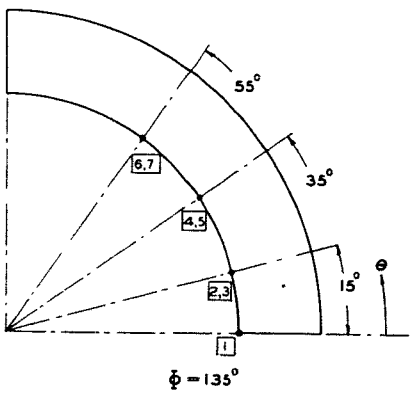

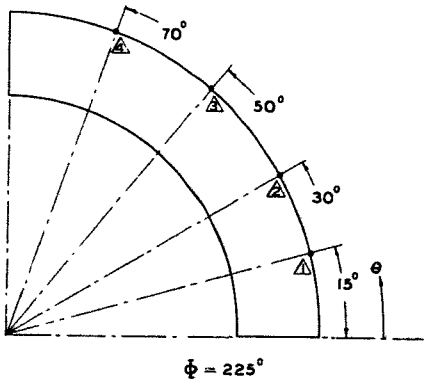

PRESSURE TAP
THERMOCOUPLE
STRAIN GAGE & ASSOC. THERMOCOUPLE

LEGEND

FIG. 1 LOCATION OF INSTRUMENTS
MODEL 2

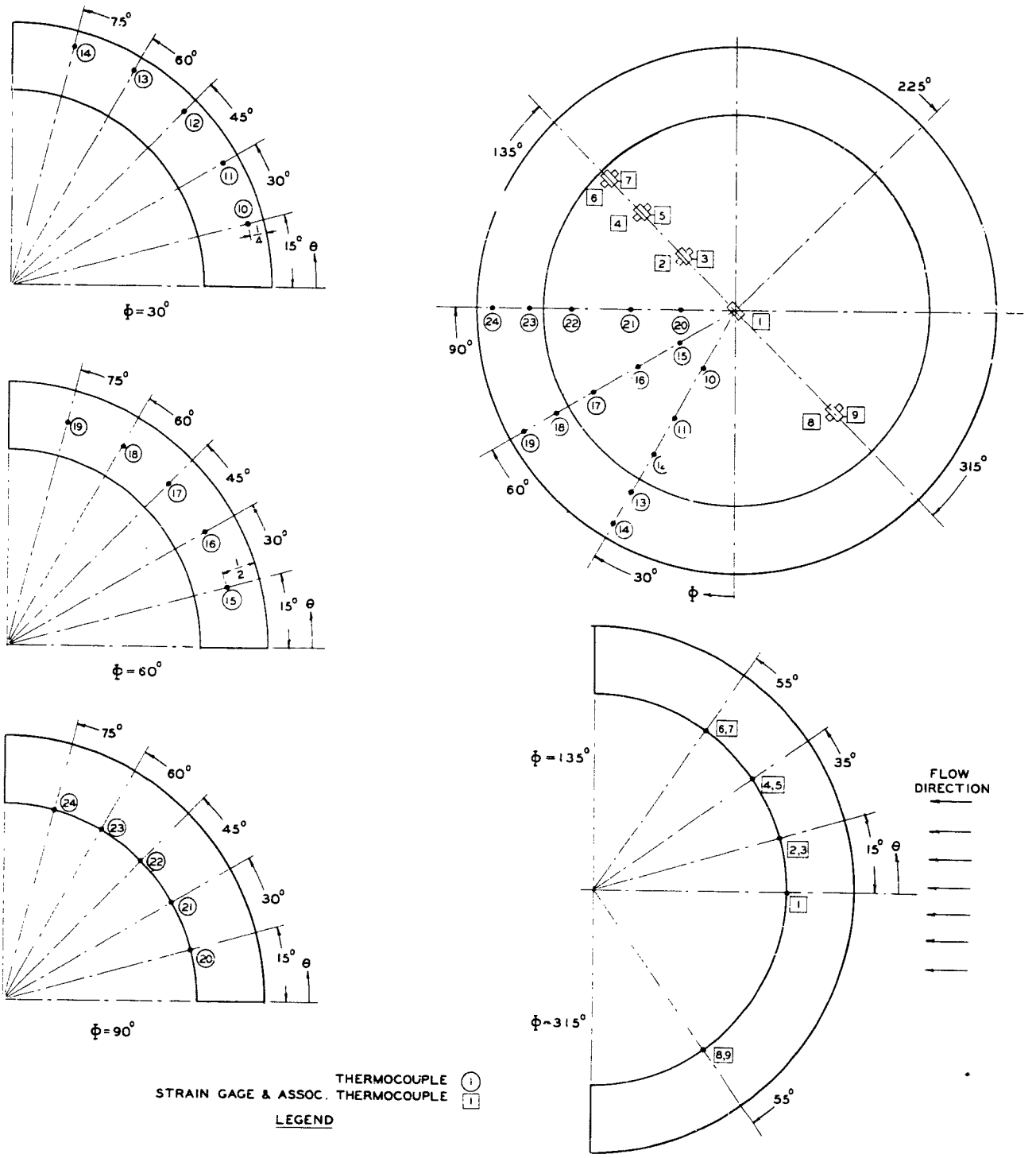

FIG. 2 LOCATION OF INSTRUMENTS
MODEL 3 .

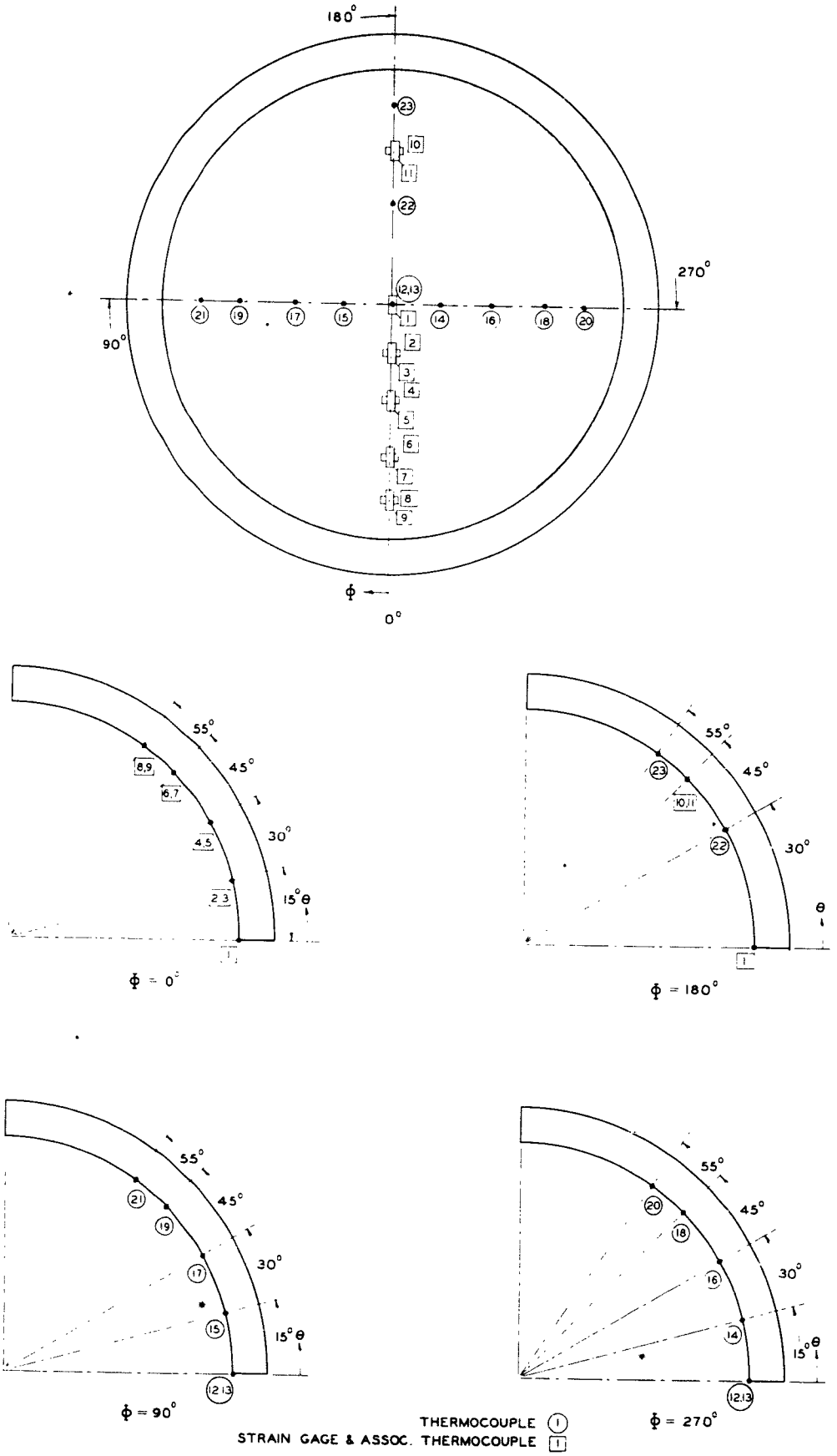

FIG. 3 LOCATION OF INSTRUMENTS
MODEL 4

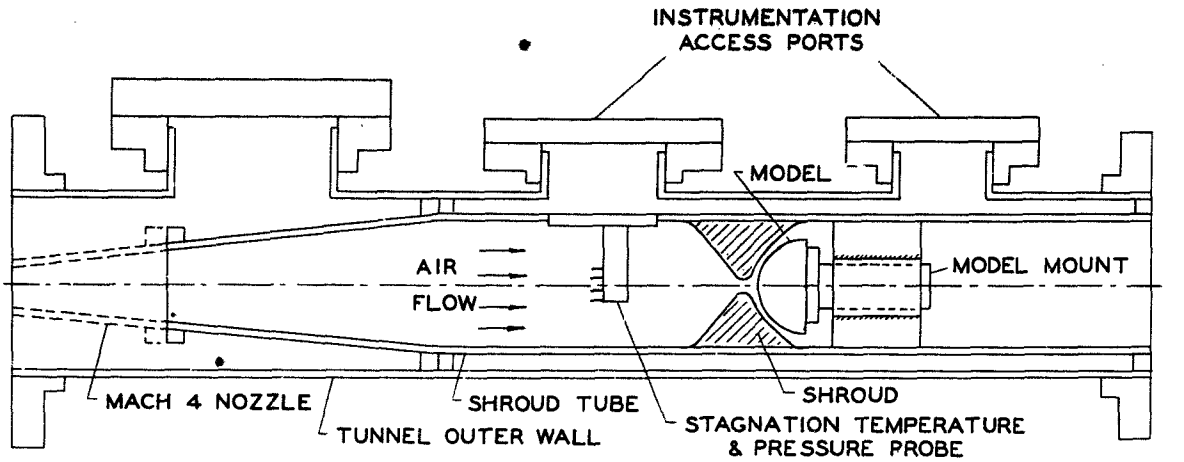

FIG. 4 SCHEMATIC SKETCH OF MODELS MOUNTED IN SHROUD TUBE

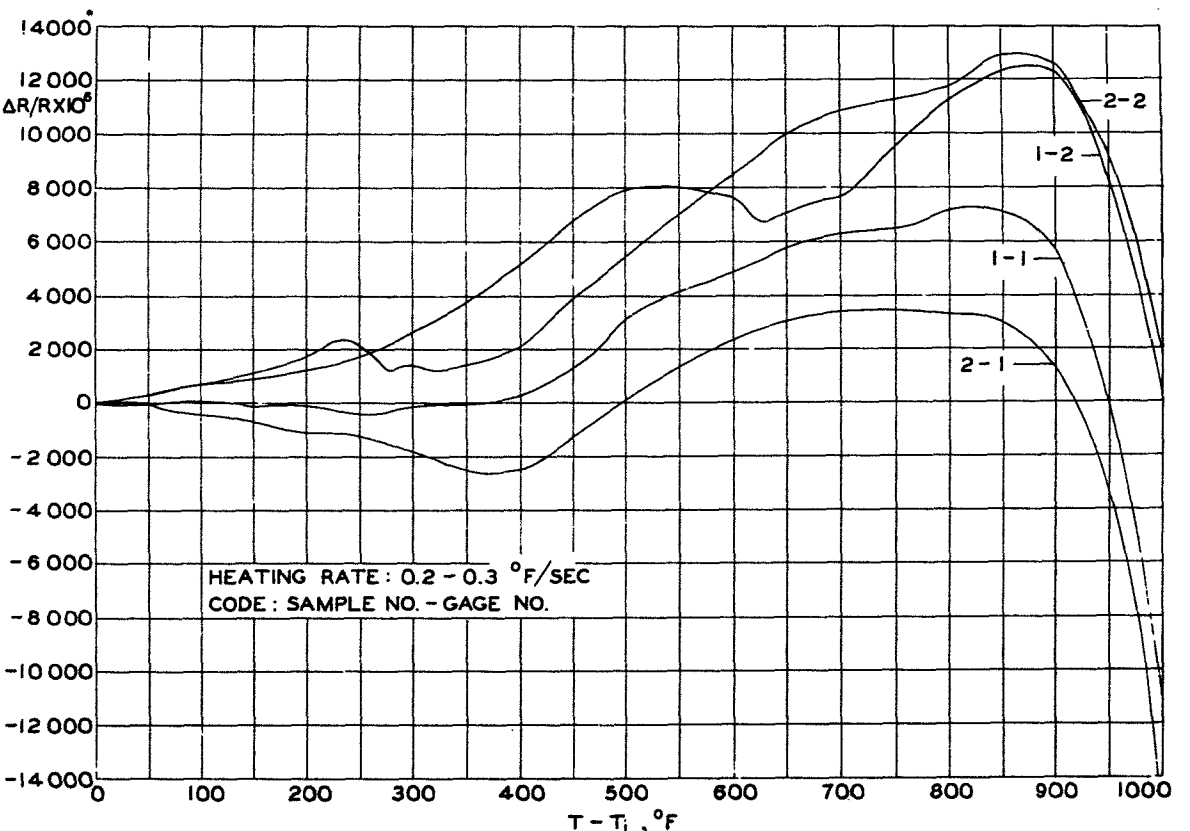

FIG. 5 STRESS-FREE TEMPERATURE RESPONSE OF HT-600 GAGES ON 356-T6 CAST ALUMINUM ALLOY SAMPLES

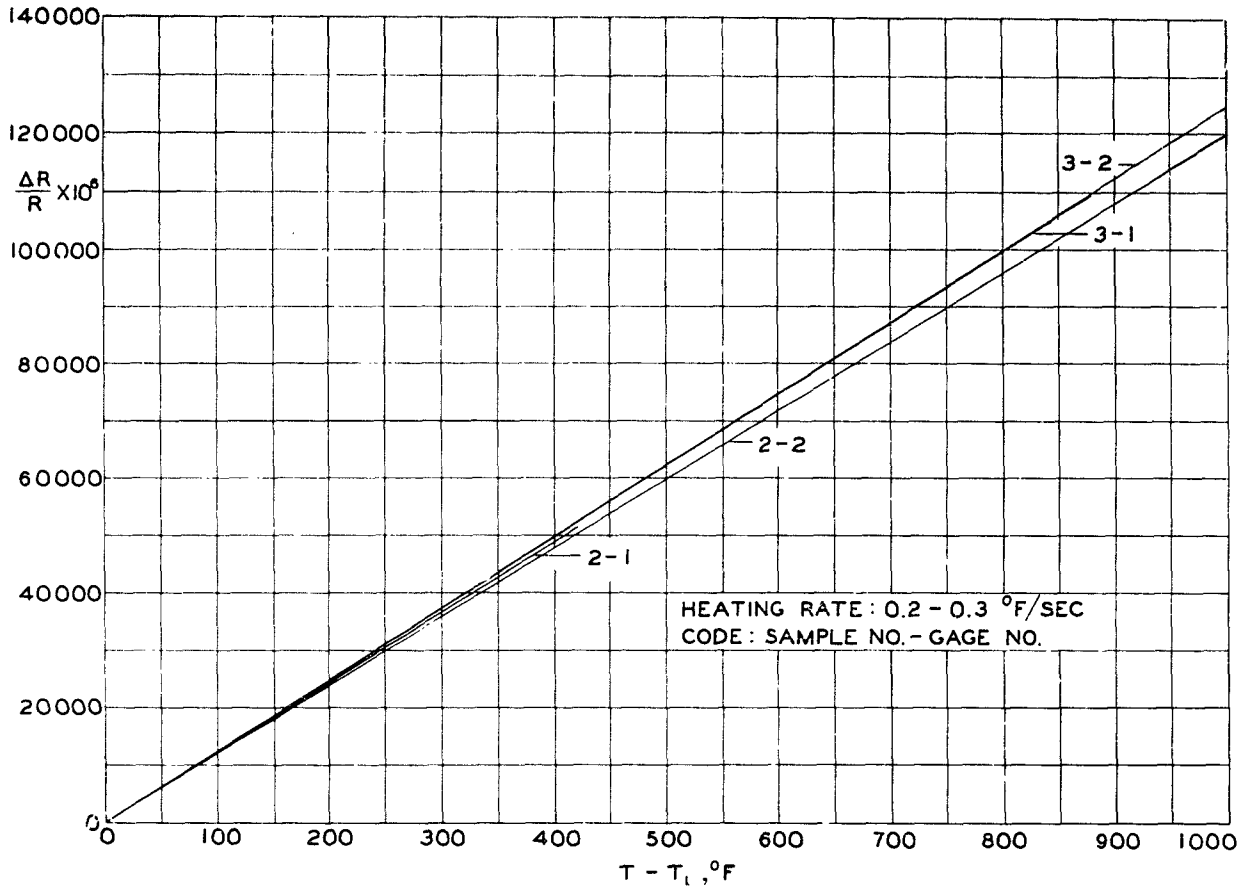

FIG. 6a STRESS-FREE TEMPERATURE RESPONSE OF HT-1200 GAGES ON 356-T6 CAST ALUMINUM ALLOY SAMPLES

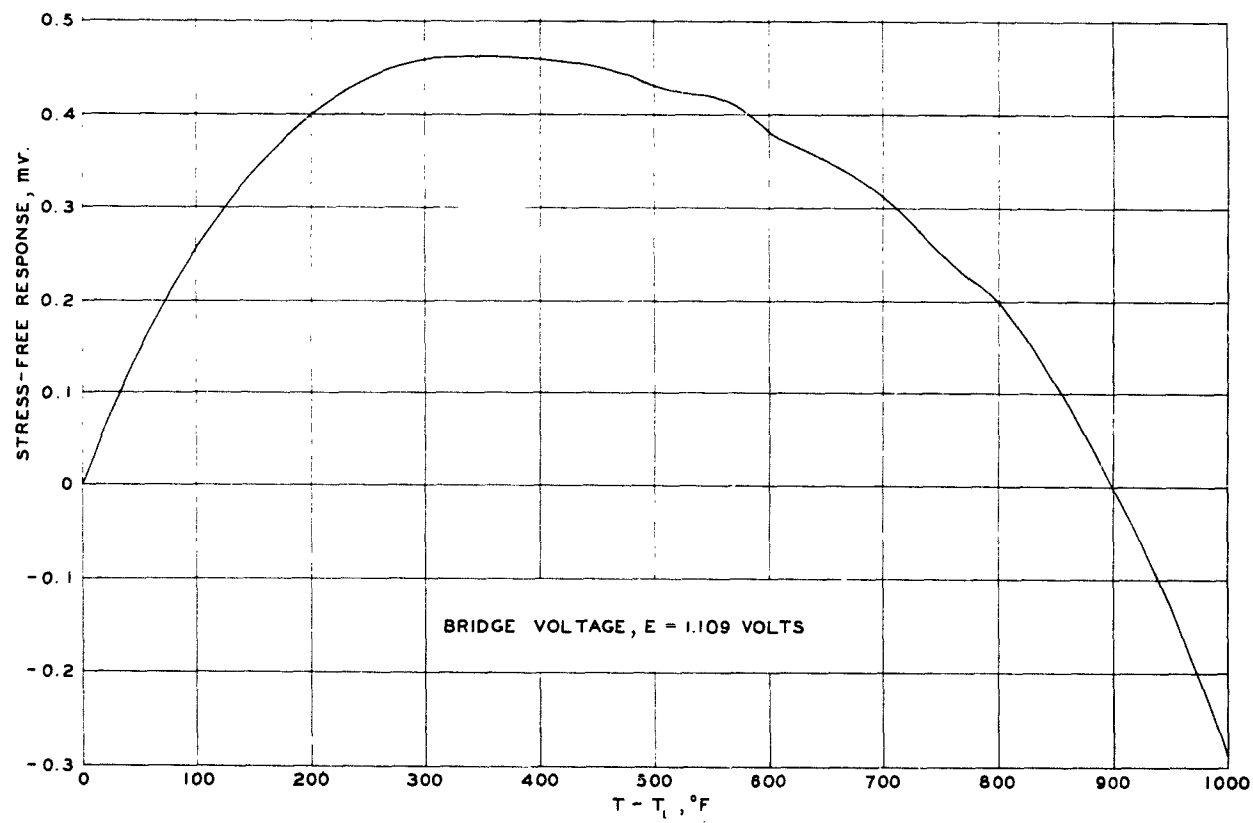

FIG. 6b STRESS-FREE TEMPERATURE RESPONSE OF AN HT-1200 GAGE ON 356 T-6 CAST ALUMINUM ALLOY SAMPLE USING T/C OUTPUT TO ATTENUATE STRAIN GAGE RESPONSE

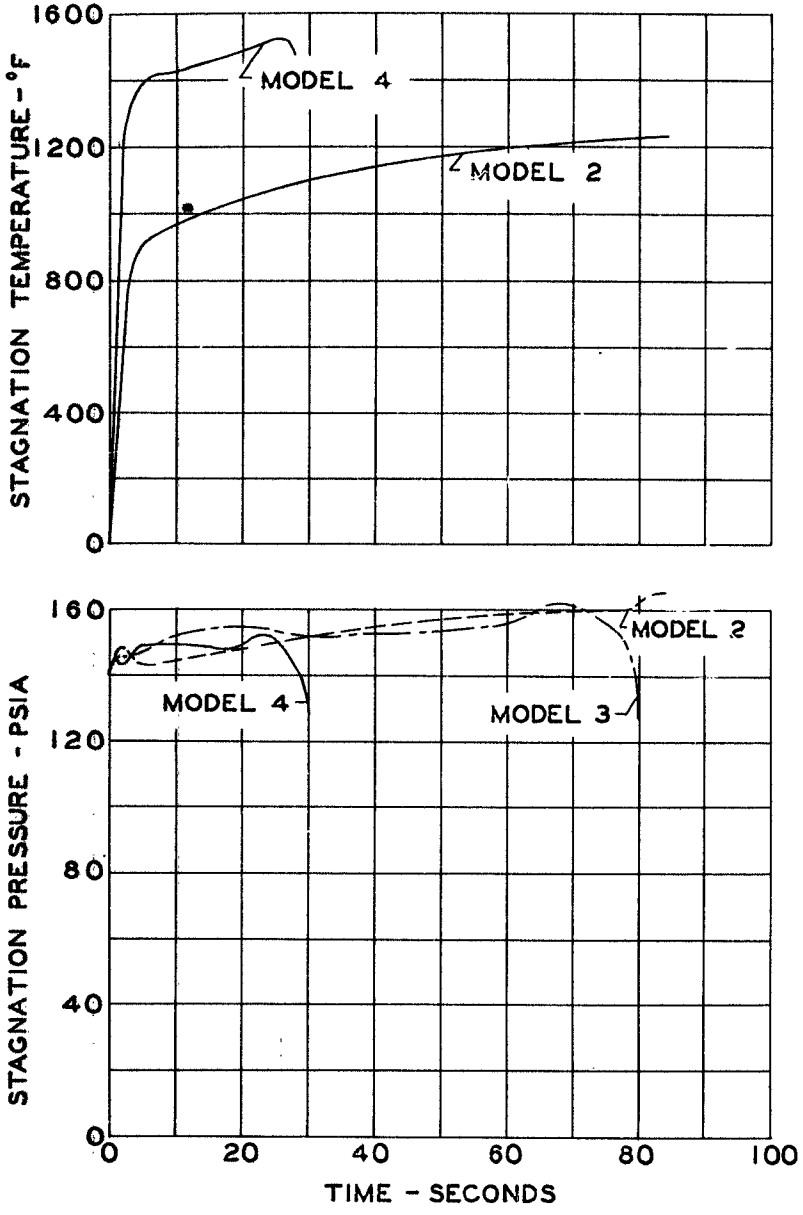

FIG. 7 WIND TUNNEL STAGNATION CONDITIONS AS A FUNCTION OF TIME

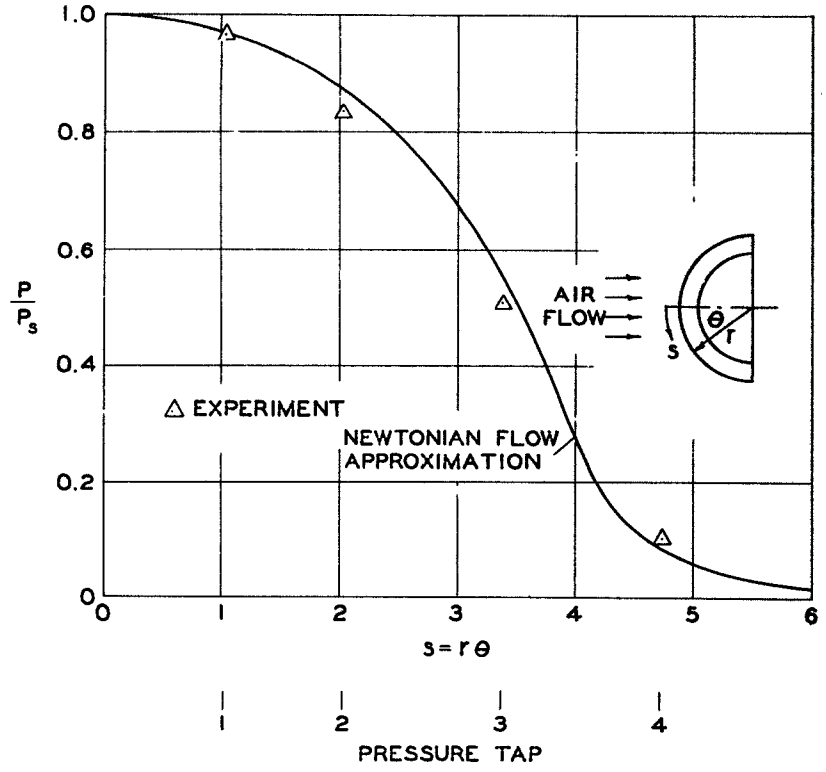

FIG. 8 PRESSURE DISTRIBUTION ON HEMISPHERICAL NOSE CONE MODEL 2

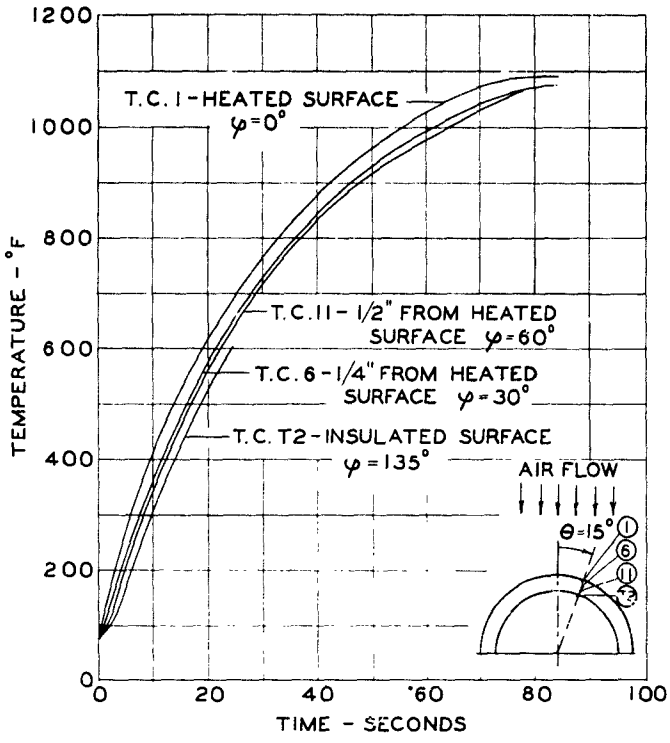

FIG. 9 TEMPERATURE-TIME HISTORIES THROUGH THICKNESS OF MODEL 2 AT $\theta = 15°$

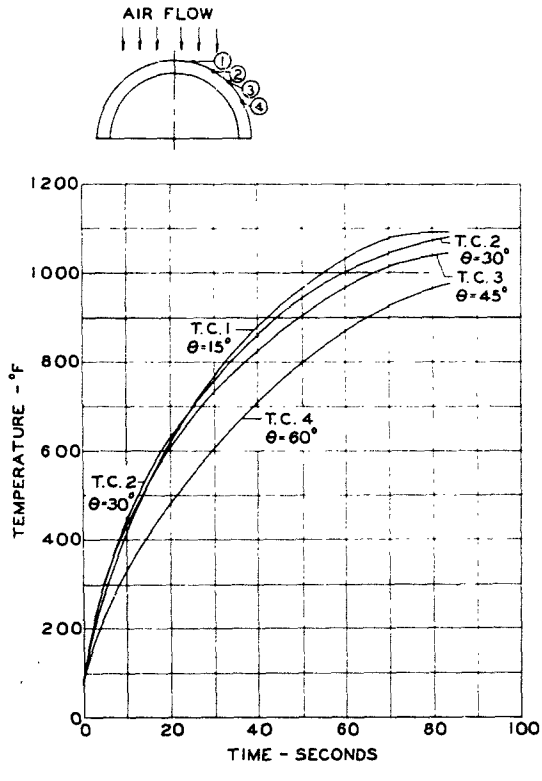

FIG. 10 TEMPERATURE-TIME HISTORIES ALONG A MERIDIAN ($\varphi = 135°$) ON HEATED SURFACE OF MODEL 2

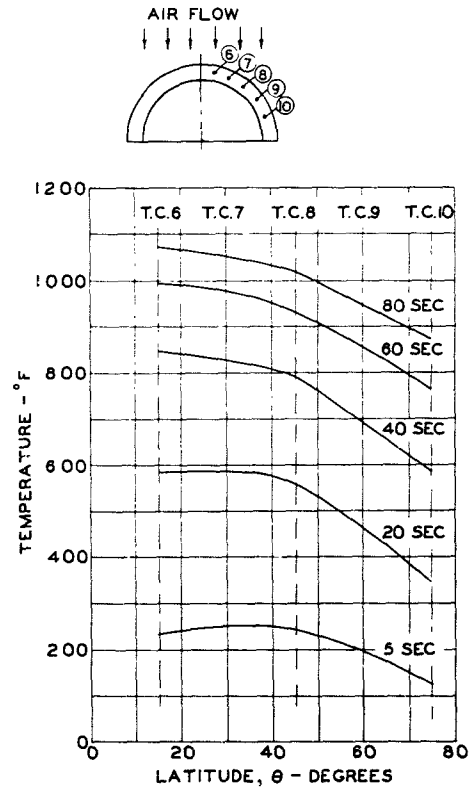

FIG. 11 TEMPERATURE DISTRIBUTION ALONG A MERIDIAN 1/4-INCH FROM HEATED SURFACE AT SELECTED TIMES - MODEL 2

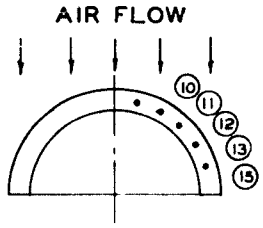

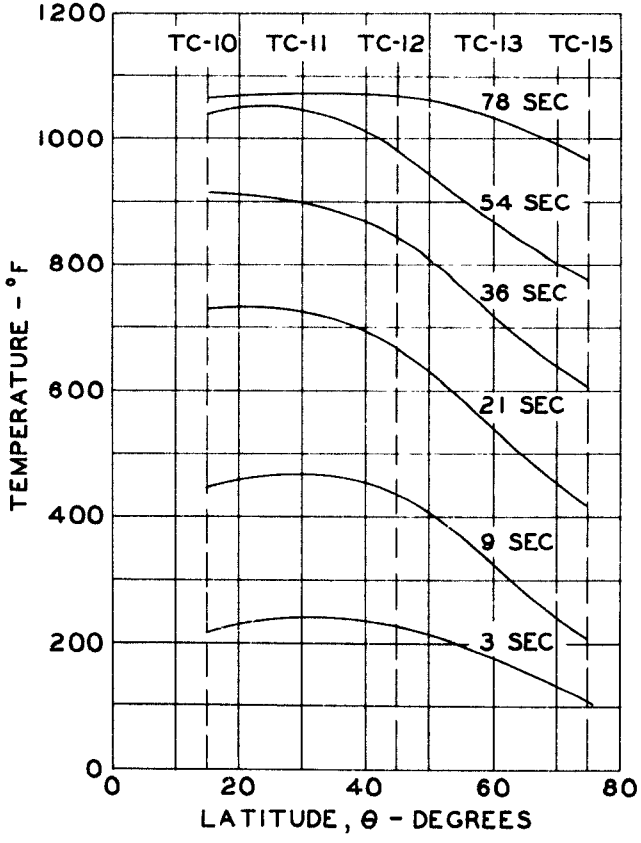

FIG. 12 TEMPERATURE DISTRIBUTION ALONG A MERIDIAN 1/4-INCH FROM HEATED SURFACE AT SELECTED TIMES - MODEL 3

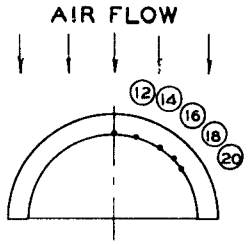

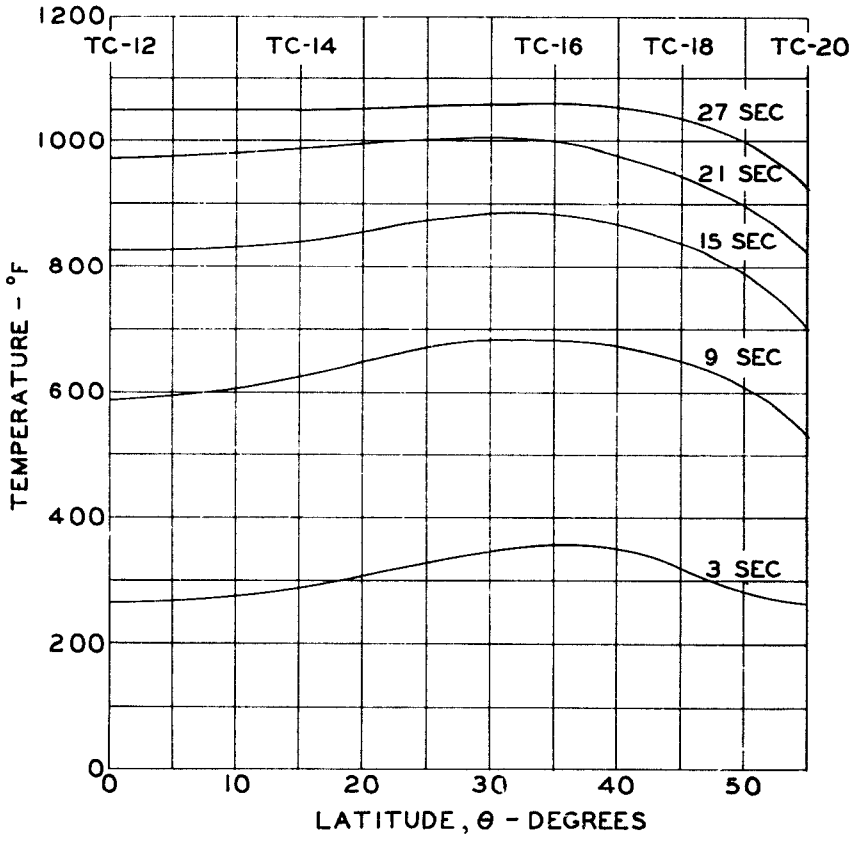

FIG. 13 TEMPERATURE DISTRIBUTION ALONG A MERIDIAN ON THE INSULATED SURFACE AT SELECTED TIMES - MODEL 4

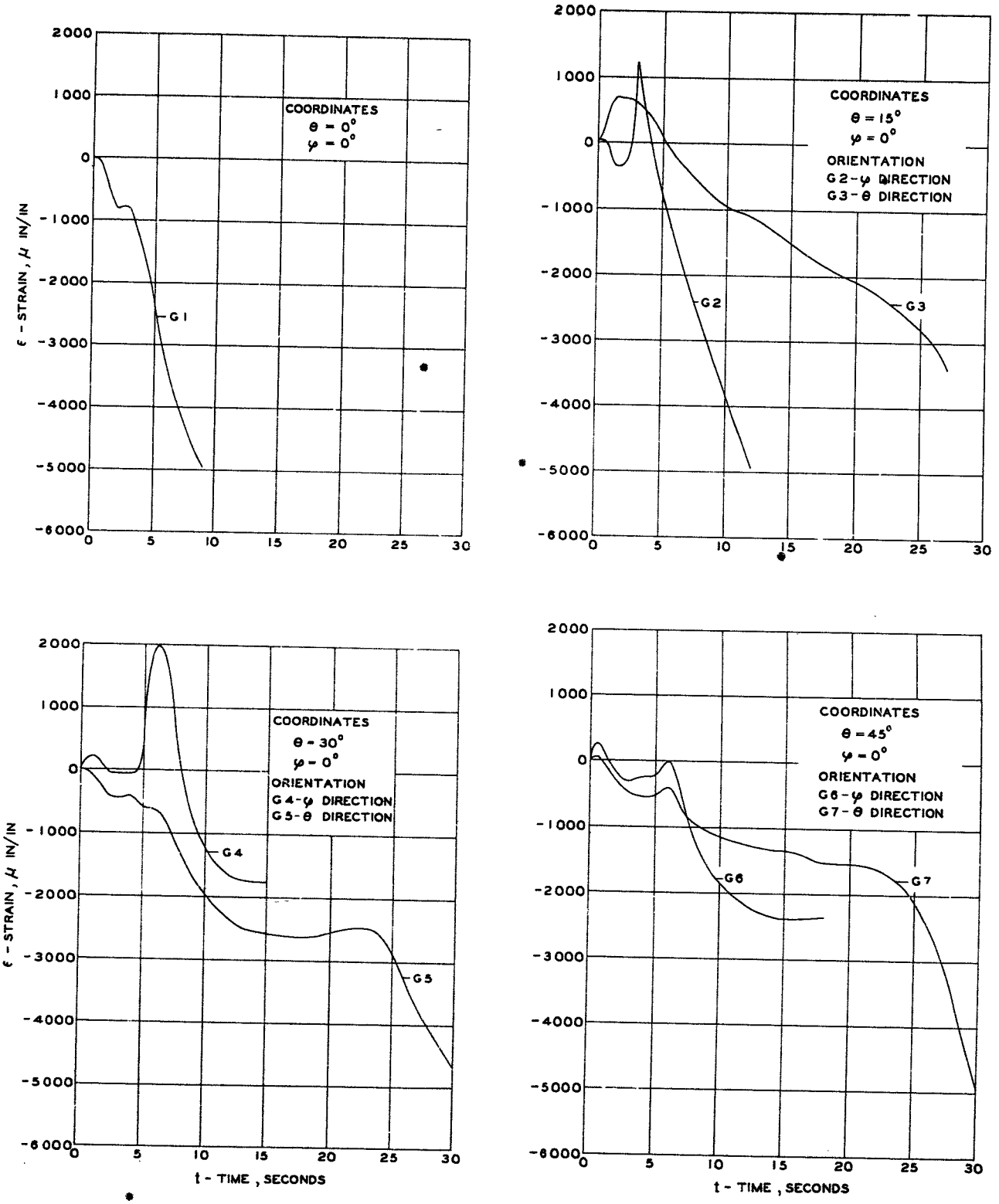

FIG. 14 STRAIN HISTORIES ON THE INSULATED SURFACE - MODEL 4

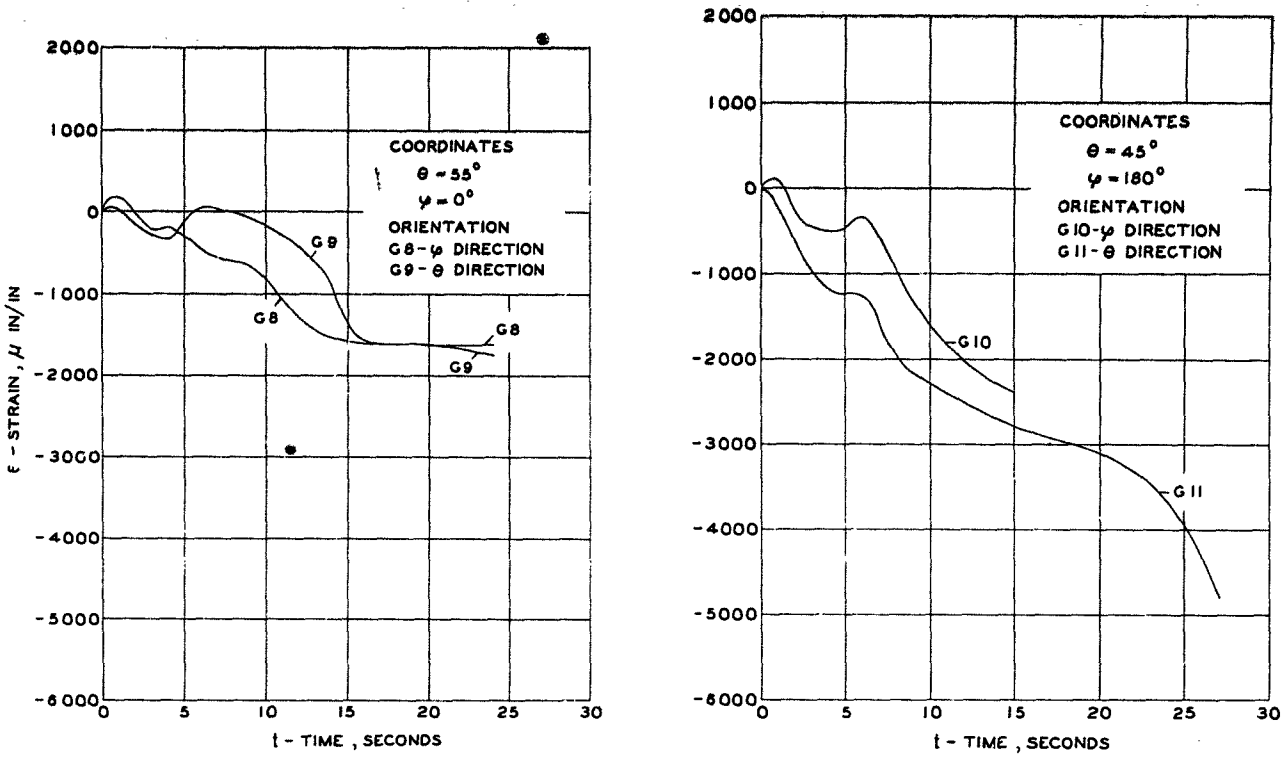

FIG. 14 STRAIN HISTORIES ON THE INSULATED SURFACE - MODEL 4

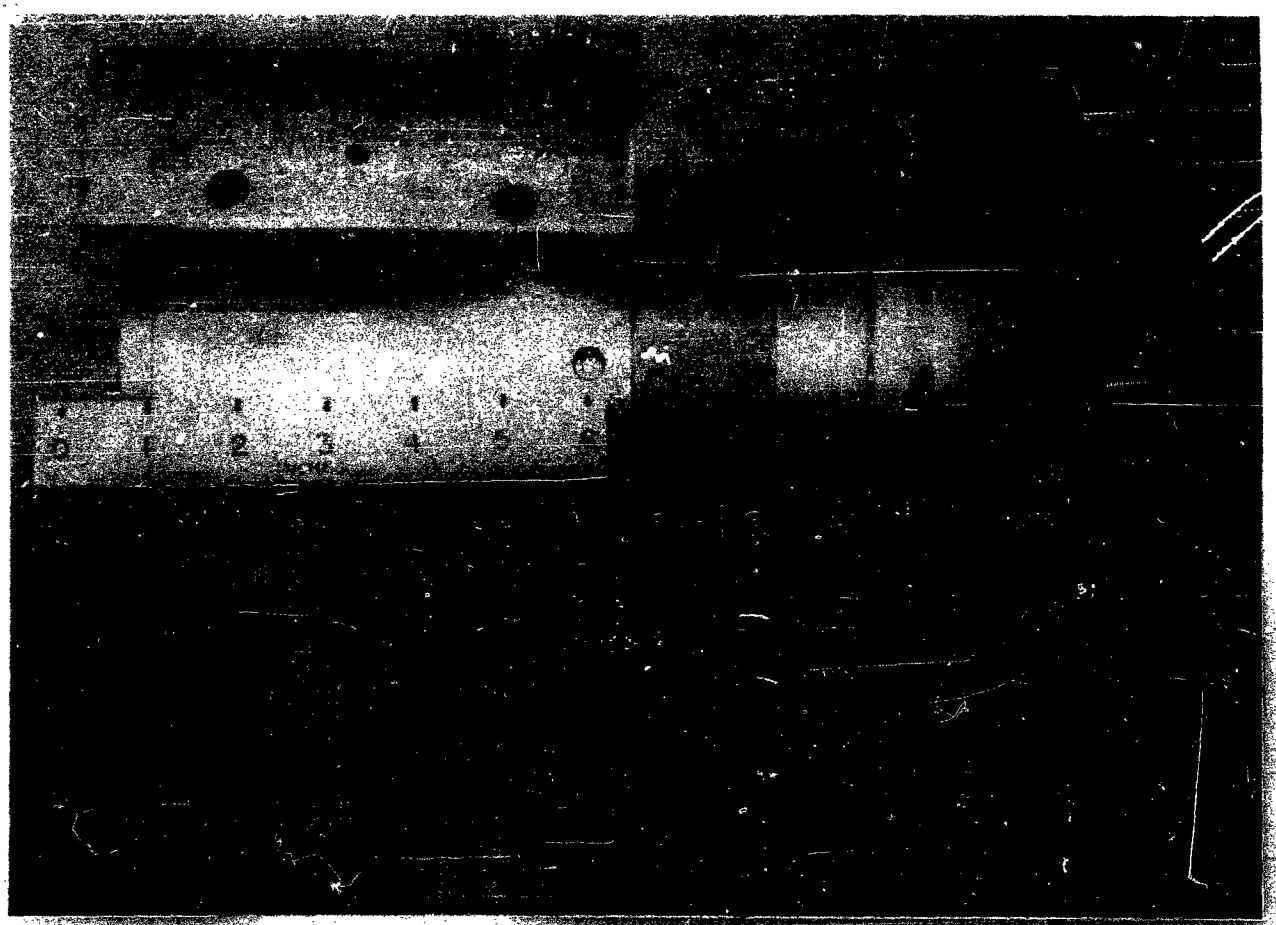

FIG. 15 SIDE VIEW OF MODEL 2 BEFORE ABLATION TEST

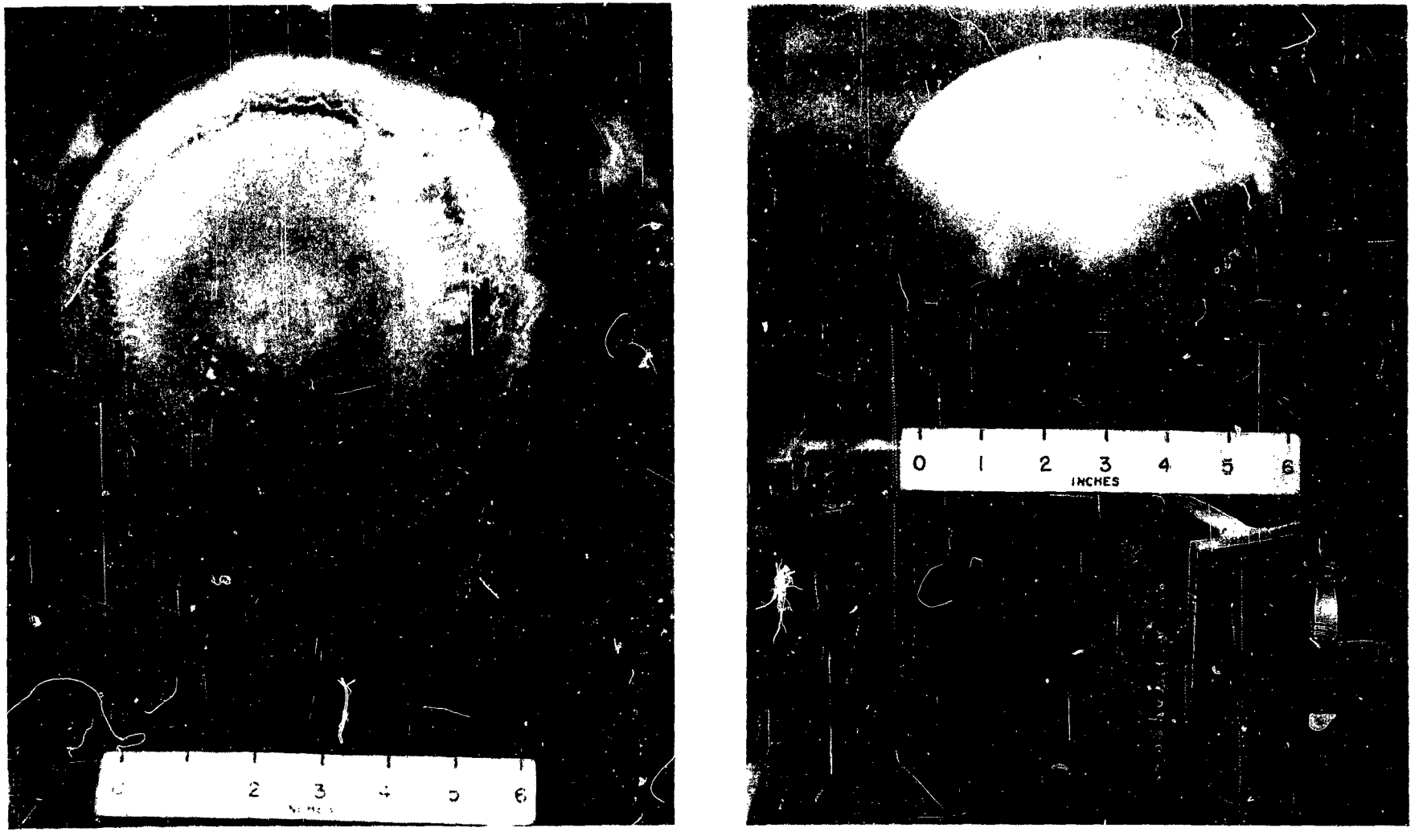

FIG. 16 FRONT AND SIDE VIEWS OF MODEL 2 AFTER TEST
STAGNATION PRESSURE : 155 PSIA
STAGNATION TEMPERATURE : 1150 °F
DURATION OF TEST : 84 SEC.

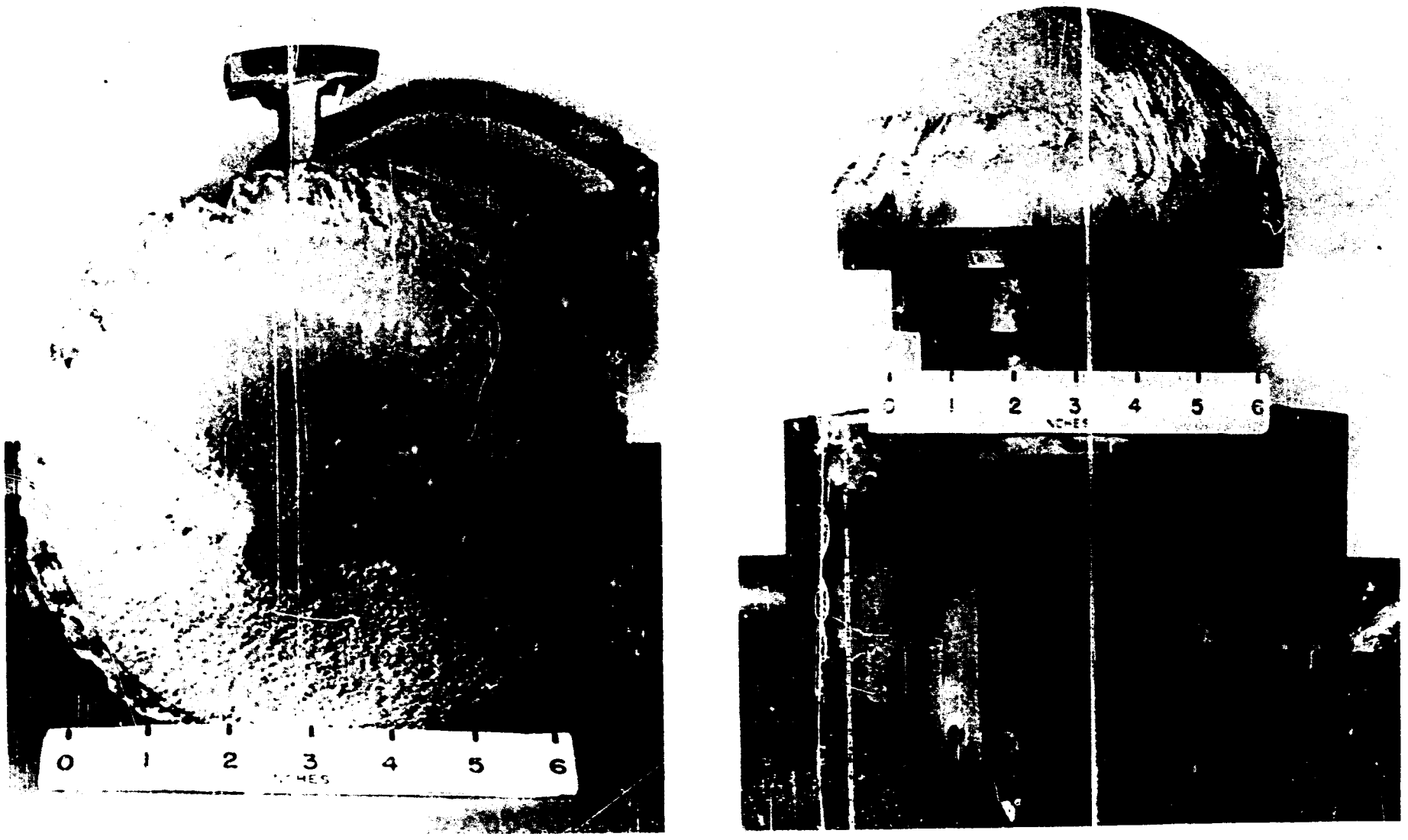

FIG. 17 FRONT AND SIDE VIEWS OF MODEL 3 AFTER TEST
STAGNATION PRESSURE : 155 PSIA
STAGNATION TEMPERATURE : 1450 °F (APPROX.)
DURATION OF TEST : 80 SEC.

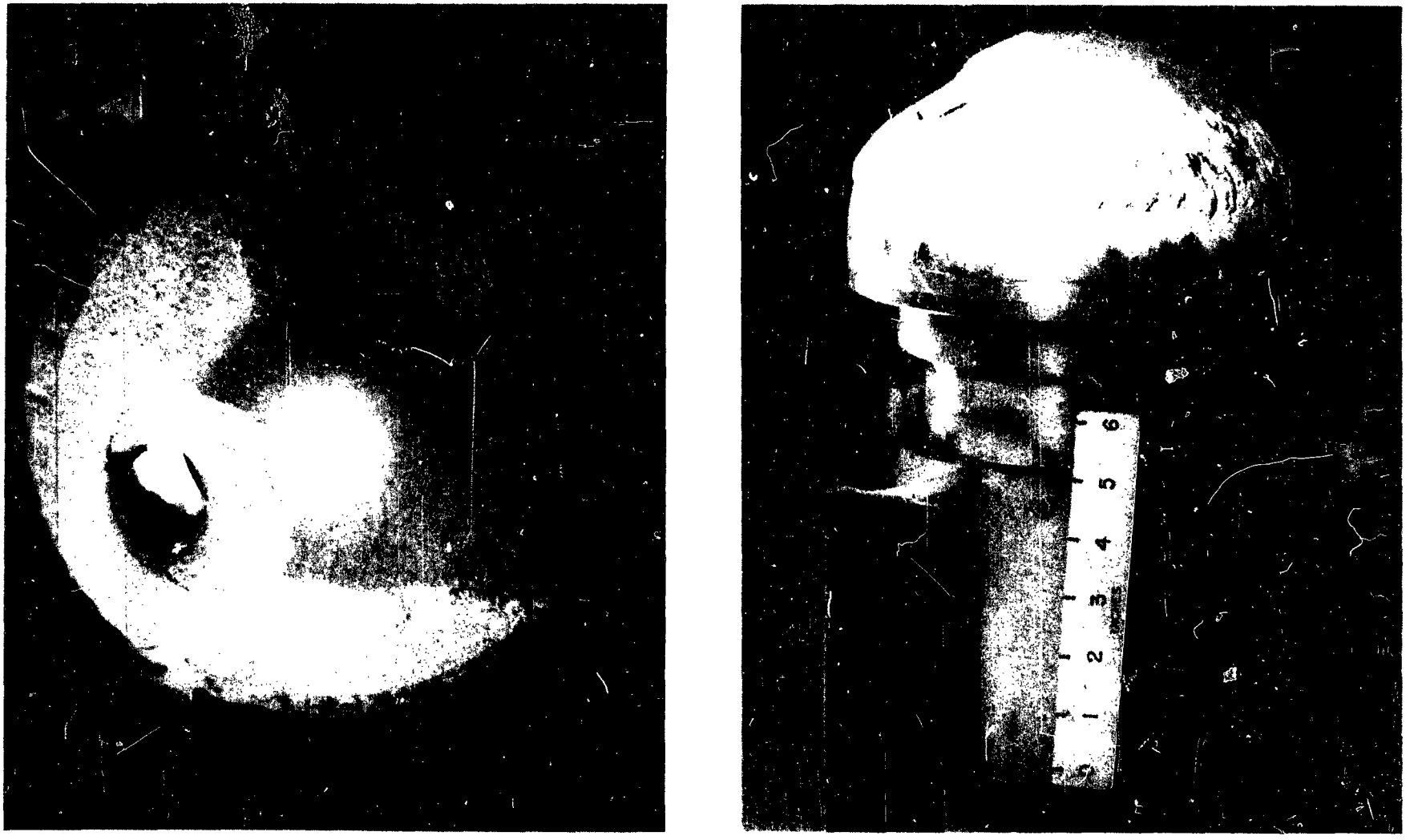

FIG. 18 FRONT AND SIDE VIEWS OF MODEL 4 AFTER TEST

STAGNATION PRESSURE : 150 PSIA
STAGNATION TEMPERATURE : 1450 °F
DURATION OF TEST : 30 SEC.

DISTRIBUTION LIST FOR UNCLASSIFIED TECHNICAL REPORTS ISSUED UNDER CONTRACT NONR 839(23), TASK NR 064-433

Chief of Naval Research
Department of the Navy
Washington 25, D.C.
Attn: Code 438 (1)
Code 439 (1)

Commanding Officer
Branch Office
Office of Naval Research
495 Summer Street
Boston 10, Massachusetts (1)

Commanding Officer
Office of Naval Research
Branch Office
John Crerar Library Building
86 E. Randolph Street
Chicago 1, Illinois (1)

Commanding Officer
Office of Naval Research
346 Broadway
New York 13, New York (1)

Commanding Officer
Office of Naval Research
Branch Office
1030 E. Green Street
Pasadena, California (1)

Commanding Officer
Office of Naval Research
Branch Office
1000 Geary Street
San Francisco, California (1)

Commanding Officer
Office of Naval Research
Navy No. 100, Fleet Post Office
New York, New York (25)

Director
Naval Research Laboratory
Washington 25, D. C.
Attn: Tech. Info. Officer (6)
Code 6200 (1)
Code 6205 (1)
Code 6250 (1)
Code 6260 (1)

Armed Services Tech. Info. Agency
Arlington Hall Station
Arlington 12, Virginia (10)

Office of Technical Services
Department of Commerce
Washington 25, D. C. (1)

Office of the Secretary of Defense
Research & Development Division
The Pentagon
Washington 25, D. C.
Attn: Technical Library (1)

Chief
Defense Atomic Support Agency
Washington 25, D. C.
Attn: Document Lib. Br. (1)

Office of the Secretary of the Army
The Pentagon
Washington 25, D. C.
Attn: ; Army Library (1)

Chief of Staff
Department of the Army
Washington 25, D. C.
Attn: Develop. Br. (R & D Div.) (1)
Research Br. (R & D Div.) (1)
Spec. Weaps. Br.
(R & D) (1)

Office of the Chief of Engineers
Department of the Army
Washington 25, D. C.
Attn: ENG-EB Prot. Const. Br., Eng. Div. Mil. Const. (1)
ENG-HL Lib. Br. Adm. Ser. Div. (1)
ENG-EA Struc. Br., Eng. Div. Mil. Const. (1)
ENG-NB Special Eng. Br. Eng. R & D Div.) (1)
ENG-WD Planning Div. Civ. Works (1)

Commanding Officer
Engineer Research Development Lab.
Fort Belvoir, Virginia (1)

Office of the Chief of Ordnance
Department of the Army
Washington 25, D. C.
Attn: Research & Materials Br. (Ord. R & D Div.) (1)

Commanding Officer
Watertown Arsenal
Watertown, Massachusetts
Attn: Laboratory Division (1)

Commanding Officer
Frankford Arsenal
Bridesburg Station
Philadelphia 37, Pennsylvania
Attn: Laboratory Division (1)

Office of Ordnance Researc h
2127 Myrtle Drive
Duke Station
Durham, North Carolina
Attn: Div. of Eng. Sciences (1)

Commanding Officer
U.S. Army Signal Res.& Dev. Lab.
SIGFM/EL-G
Fort Monmouth, New Jersey (1)

Chief of Naval Operations
Department of the Navy
Washington 25, D. C.
Attn: Op 37 (1)

Commandant Marine Corps
Headquarters, U.S. Marine Corps
Washington 25, D. C. (1)

Chief, Bureau of Ships
Department of the Navy
Washington 25, D. C.
Attn: Code 312 (2)
Code 376 (1)
Code 377 (1)
Code 420 (1)
Code 423 (2)
Code 442 (2)

Chief, Bureau of Aeronautics
Department of the Navy
Washington 25, D. C.
Attn: AE-4 (1)
AV-34 (1)
AD (1)
AD-2 (1)
RS-7 (1)
RS-8 (1)
SI (1)
TS-42 (1)

Chief, Bureau of Ordnance
Department of the Navy
Washington 25, D.C.
Attn: Ad 3 (1)
Re (1)
Res (1)
Reu (1)
ReS5 (1)
ReS1 (1)
Ren (1)

Special Projects Office
Bureau of Ordnance
Department of the Navy
Washington 25, D.C.
Attn: Missile Branch (2)

Chief, Bureau of Yards & Docks
Department of the Navy
Washington 25, D.C.
Attn: Code D-202 (1)
Code D-202.3 (1)
Code D-220 (1)
Code D-222 (1)
Code D-410C (1)
Code D-440 (1)
Code D-500 (1)

Commanding Officer & Director
David Taylor Model Basin
Washington 7, D. C.
Attn: Code 140 (1)
Code 600 (1)
Code 700 (1)
Code 720 (1)
Code 725 (1)
Code 731 (1)
Code 740 (2)

Commander
U.S. Naval Ordnance Laboratory
White Oak, Maryland
Attn: Technical Library (2)
Technical Evaluation Dep. (1)

Director
Materials Laboratory
New York Naval Shipyard
Brooklyn 1, New York (1)

Commanding Officer & Director
U.S. Naval Electronics Lab.
San Diego 52, California (1)

Officer-in-Charge
Naval Civil Engineering Research
and Evaluation Laboratory
U.S. Naval Construction
Battalion Center
Port Hueneme, California (2)

Director
Naval Air Experimental Station
Naval Air Material Center
Naval Base
Philadelphia 12, Pennsylvania
Attn: Materials Laboratory (1)
Structures Laboratory (1)

Officer-in-Charge
Underwater Explosion Research Div.
Norfolk Naval Shipyard
Portsmouth, Virginia
Attn: Dr. A.H. Keil (2)

Commander
U.S. Naval Proving Grounds
Dahlgren, Virginia (1)

Commander
Naval Ordnance Test Station
Inyokern, China Lake, California
Attn: Physics Division (1)
Mechanics Branch (1)

Commander
Naval Ordnance Test Station
Underwater Ordnance Division
3202 E. Foothill Boulevard
Pasadena 8, California
Attn: Structures Division (1)

Commanding Officer & Director
Naval Engineering Experiment Station
Anapolis, Maryland

Superintendent
Naval Post Graduate School
Monterey, California (1)

Commandant
Marine Corps Schools
Quantico, Virginia
Attn: Director, Marine Corps
Development Division (1)

Commanding General
U.S. Air Force
Washington 25, D.C.
Attn: Research & Devel. Div. (1)

Commander
Air Material Command
Wright-Patterson Air Force Base
Dayton, Ohio
Attn: MCREX-B (1)
Structures Division (1)

Commander
U.S. Air Force Institute of Tech.
Wright-Patterson Air Force Base
Dayton, Ohio=
Attn: Chief, Applied Mechanics
Group (1)

Director of Intelligence
Headquarters, U.S. Air Force
Washington 25, D.C.
Attn: P.V. Branch
(Air Targets Division)(1)

Commander
Air Force Office of Scientific Res.
Washington 25, D.C.
Attn: Mechanics Division (1)

U.S. Atomic Energy Commission
Washington 25, D.C.
Attn: Director of Research (2)

Director
National Bureau of Standards
Washington 25, D.C.
Attn: Division of Mechanics (1)
Engineering Mechs. Sect.(1)
Aircraft Structures (1)

Commandant
U.S. Coat Gurad
1300 E Street, N.W.
Washington 25, D.C.
Attn: Chief, Testing & Devel.
Division (1)

U.S. Maritime Administration
General Admin. Office Building
Washington 25, D.C.
Attn: Chief, Div. of Preliminary
Design (1)

National Aeronautics & Space
Administration
1512 H Street, N.W.
Washington 25, D.C.
Attn: Loads & Structures Div. (2)

Director
Langley Aeronautical Laboratory
Langley Field, Virginia
Attn: Structures (2)

Director
Forest Products Laboratory
Madison, Wisconsin (1)

Civil Aeronautics Administration
Department of Commerce
Washington 25, D.C.
Attn: Chief, Aircraft Engineering
Div. (1)
Chief, Airframe & Equipment
D (1)

Professor Lynn S. Beedle
Fritz Engineering Laboratory
Lehigh University
Bethlehem, Pennsylvania (1)

Professor R. L. Bisplinghoff
Dept. of Aeronautical Engineering
Massachusetts Inst. of Technology
Cambridge 39, Massachusetts (1)

Professor H. H Bleich
Department of Civil Engineering
Columbia University
New York 27, New York

Professor B. A. Boley
Department of Civil Engineering
Columbia University
New York 27, New York

National Sciences Foundation
1520 H Street, N.W.
Washington, D.C.
Attn: Engineering Sciences Division(1)

Professor G. F. Carrier
Pierce Hall
Harvard University
Cambridge 38, Massachusetts

National Academy of Sciences
2101 Constitution Avenue
Washington 25, D.C.
Attn: Tech. Director, Comm. on Ships' Structural Design
Exec. Sec'ty, Comm. on Undersea Warfare (1)

Professor Herbert Deresciewicz
Dept. of Civil Engineering
Columbia University
632 W. 125th Street
New York 27, New York (1)

Professor D.C. Drucker, Chairman
Divison of Engineering
Brown University
Providence, Rhode Island (1)

Professor A.C. Eringen
Dept. of Aeronautical Engineering
Purdue University
Lafayette, Indiana (1)

Professor W. Flugge
Dept. of Mechanical Engineering
Stanford University
Stanford, California (1)

Professor J. N. Goodier
Dept. of Mechanical Engineering
Stanford University
Stanford, California (1)

Professor L.E. Goodman
Engineering Experiment Station
University of Minnesota
Minneapolis, Minnesota (1)

Professor M. Hetenyi
The Technological Institute
Northwestern University
Evanston, Illinois (1)

Professor P.G. Hodge, Jr.
Dept. of Mechanics
Technology Center
Illinois Inst. of Technology
Chicago 16, Illinois (1)

Professor N.J. Hoff, Head
Division of Aeronautical Engrg.
Stanford University
Stanford, California (1)

Professor W.H. Hoppmann, II
Dept. of Mechanics
Rensselaer Polytechnic Inst.
Troy, New York (1)

Professor Bruce G. Johnston
University of Michigan
Ann Arbor, Michigan (1)

Professor J. Kempner
Dept. of Aerospace Engrg. and Applied Mechanics
Polytechnic Institute of B'klyn.
333 Jay Street
Brooklyn 1, New York (1)

Professor H.L. Langhaar
Dept. of Theoretical and Appl. Mech.
University of Illinois
Urbana, Illinois (1)

Professor B.J. Lazan, Director
Engineering Experiment Station
University of Minnesota
Minneapolis 14, Minnesota (1)

Professor E.H. Lee
Division of Applied Mathematics
Brown University
Providence 12, Rhode Island (1)

Professor George H. Lee
Director of Research
Rensselaer Polytechnic Institute
Troy, New York (1)

Mr. M.M. Lemcoe
Southwest Research Institute
8500 Culebra Road
San Antonio 6, Texas (1)

Professor Paul Lieber
Geology Department
University of California
Berkeley 4, California (1)

Professor R.D. Mindlin
Dept. of Civil Engineering
Columbia University
632 W. 125th Street
New York 27, New York (1)

Professor Paul M. Naghdi
Building T-7
College of Engineering
University of California
Berkeley 4, California (1)

Professor William A. Nash
Dept. of Engineering Mechanics
University of Florida
Gainesville, Florida (1)

Professor N.M. Newmark, Head
Dept. of Civil Engineering
University of Illinois
Urbana, Illinois (1)

Professor Aris Phillips
Dept. of Civil Engineering
15 Prospect Street
Yale University
New Haven, Connecticut (1)

Professor W. Prager, Chairman
Physical Sciences Council
Brown University
Providence 12, Rhode Island (1)

Professor E. Reissner
Dept. of Mathematics
Massachusetts Inst. of Technology
Cambridge 39, Massachusetts (1)

Professor M.A. Sadowsky
Dept. of Mechanics
Rensselaer Polytechnic Institute
Troy, New York (1)

Professor J. Stallmeyer
Dept of Civil Engineering
University of Illinois
Urbana, Illinois (1)

Professor Eli Sternberg
Dept. of Mechanics
Brown University
Providence 12, Rhode Island (1)

Professor S.P. Timoshenko
School of Engineering
Stanford University
Stanford, California (1)

Professor A.S. Velestos
Dept. of Civil Engineering
University of Illinois
Urbana, Illinois (1)

Professor Dana Young
Yale University
New Haven, Connecticut (1)

Dr. John F. Brahtz
Dept. of Engineering
University of California
Los Angeles, California (1)

Mr. Martin Goland, Vice President
Southwest Research Institute
8500 Culebra Road
San Antonio, Texas (1)

Mr. S. Levy
General Electric Research Lab.
6901 Elmwood Avenue
Philadelphia 42, Pa. (1)

Professor B. Budiansky
Dept. of Mechanical Engineering
School of Applied Sciences
Harvard University
Cambridge 38, Massachusetts (1)

Professor H. Kolsky
Division of Engineering
Brown University
Providence 12, Rhode Island (1)

Professor E. Orowan
Department of Mechanical Engrg.
Mass. Institute of Technology
Cambridge 39, Massachusetts (1)

Professor J. Ericksen
Mechanical Engrg. Department
John Hopkins University
Baltimore 18, Maryland (1)

Professor T.Y. Thomas
Graduate Institute for Mathematics
and Mechanics
Indiana University
Bloomington, Indiana (1)

Professor Joseph Martin, Head
Dept. of Engineering Mechanics
College of Engrg. and Architecture
Pennsylvania State University
University Park, Pennsylvania (1)

Mr. K.H. Koopman, Secretary
Welding Research Council of
The Engineering Foundation
29 West 39th Street
New York 18, New York (2)

Professor Walter T. Daniels
School of Engrg. and Architecture
Howard University
Washington 1, D.C. (1)

Dr. D.O. Brush
Structures Department 53-13
Lockheed Aircraft Corporation
Missile Systems Division
Synnyvale, California (1)

Professor Nicholas Perrone
Engineering Science Dept.
Pratt Institute
Brooklyn 5, New York (1)

Legislative Reference Service
Library of Congress
Washington 25, D.C.
Attn: Dr. E. Wenk (1)

Commander
Wright Air Development Center
Wright-Patterson Air Force Base
Dayton, Ohio
Attn: Dynamics Branch (1)
Aircraft Laboratory (1)
WCISY (1)

Commanding Officer
USNNOEU
Kirtland Air Force Base
Albuquerque, New Mexico
Attn: Code 20 (Dr. J.N. Brennan) (1)

Professor J.E. Cermak
Dept. of Civil Engineering
Colorado State University
Fort Collins, Colorado (1)

Professor W.J. Hall
Dept. of Civil Engineering
University of Illinois
Urbana, Illinois (1)

Project Staff (10)

For your future distribution (10)